On Electric Currents in Sunspots

P. Venkatakrishnan

Currents in Astrophysical Plasma

- Current is created by confining flows of the plasma in the form of j= $\nabla \times \boldsymbol{B}$
- The electric field in the frame of the moving plasma, E = j/s given by Ohm's law, will be negligibly small on account of high conductivity
- In a flux-tube carrying a current, the field must decrease as 1/r outside the tube.
- If the flux-tube is confined by field free plasma, then it must necessarily have zero net current
- A bunch of current free tubes will have zero net current

On The Absence Of Photospheric Net Currents In Vector Magnetograms Of Sunspots Obtained From *Hinode*

P. Venkatakrishnan and Sanjiv Kumar Tiwari
Udaipur Solar Observatory, Physical Research Laboratory, Dewali, Bari Road,
Udaipur-313 001, India; pvk@prl.res.in, stiwari@prl.res.in

The Astrophysical Journal, **706**: L114–L119, 2009 November 20

Following Parker (1996), we consider a long straight flux bundle surrounded by a region of field-free plasma.
The vertical component of the electric current density consists of two terms, viz.,

$$-\frac{1}{\mu_0 r}\frac{\partial B_r}{\partial \psi} \text{ and } \frac{1}{\mu_0 r}\frac{\partial (r B_\psi)}{\partial r}.$$

We will call the first term as the "pleat current density," and the second term as the "twist current density,"
The net current *Iz* within a distance ϖ from the center is then given by

$$I_z(\varpi) = \int_0^{2\pi} d\psi \int_0^{\varpi} r dr (j_p + j_t). \qquad (1)$$

The ψ integral over j_p vanishes, while the second term yields

$$I_z(\varpi) = \frac{\varpi}{\mu_0} \int d\psi B_\psi(\varpi, \psi) \qquad (2)$$

THE DATA SETS AND ANALYSIS

•We have analyzed the vector magnetograms obtained from SOT/SP

•The calibration of data sets have been performed using the standard "sp_prep" routine developed by B. Lites and available in the Solar-Soft package.

•The prepared polarization spectra have been inverted to obtain vector magnetic field components using an Unno–Rachkowsky inversion under the assumption of Milne–Eddington (ME) atmosphere.

•We have used the inversion code "Stokesfit.pro" which has been kindly made available by T. R. Metcalf as a part of the Solar-Soft package.

•In order to minimize the noise, pixels with transverse (*Bt*) and longitudinal magnetic field (*Bz*) greater than a certain level are only analyzed.

•The data sets with their observation details are given in Table 1.

•We have studied only those spots where the polarity inversion lines are well separated from the edge of the sunspot.

The results of the inversions yield the three magnetic parameters, viz., the field strength *B*, the inclination to the line of sight γ , and the azimuth φ.
These parameters are used to obtain the three components of magnetic field in Cartesian geometry as

$$B_z = B\cos\gamma,$$

$$B_y = B\sin\gamma\sin\phi,$$

$$B_x = B\sin\gamma\cos\phi.$$

The transverse vector is then expressed in cylindrical geometry as

$$B_r = \frac{1}{r}(x B_x + y B_y),$$

$$B_\psi = \frac{1}{r}(-y B_x + x B_y).$$

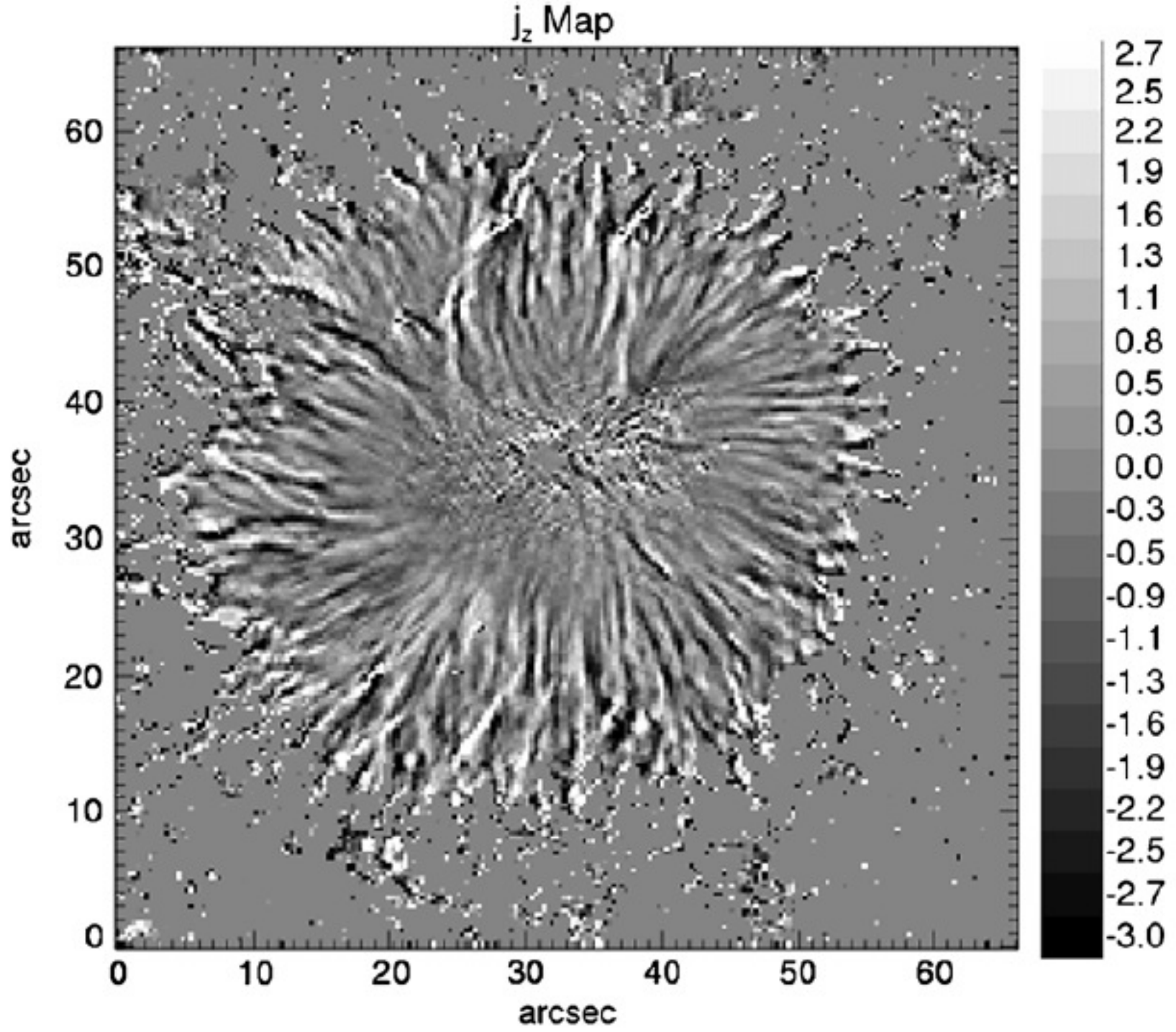
j_z Map
arcsec
arcsec
0
10
20
30
40
50
60
2.7
2.5
2.2
1.9
1.6
1.3
1.1
0.8
0.5
0.3
0.0
-0.3
-0.5
-0.9
-1.1
-1.3
-1.6
-1.9
-2.2
-2.5
-2.7
-3.0

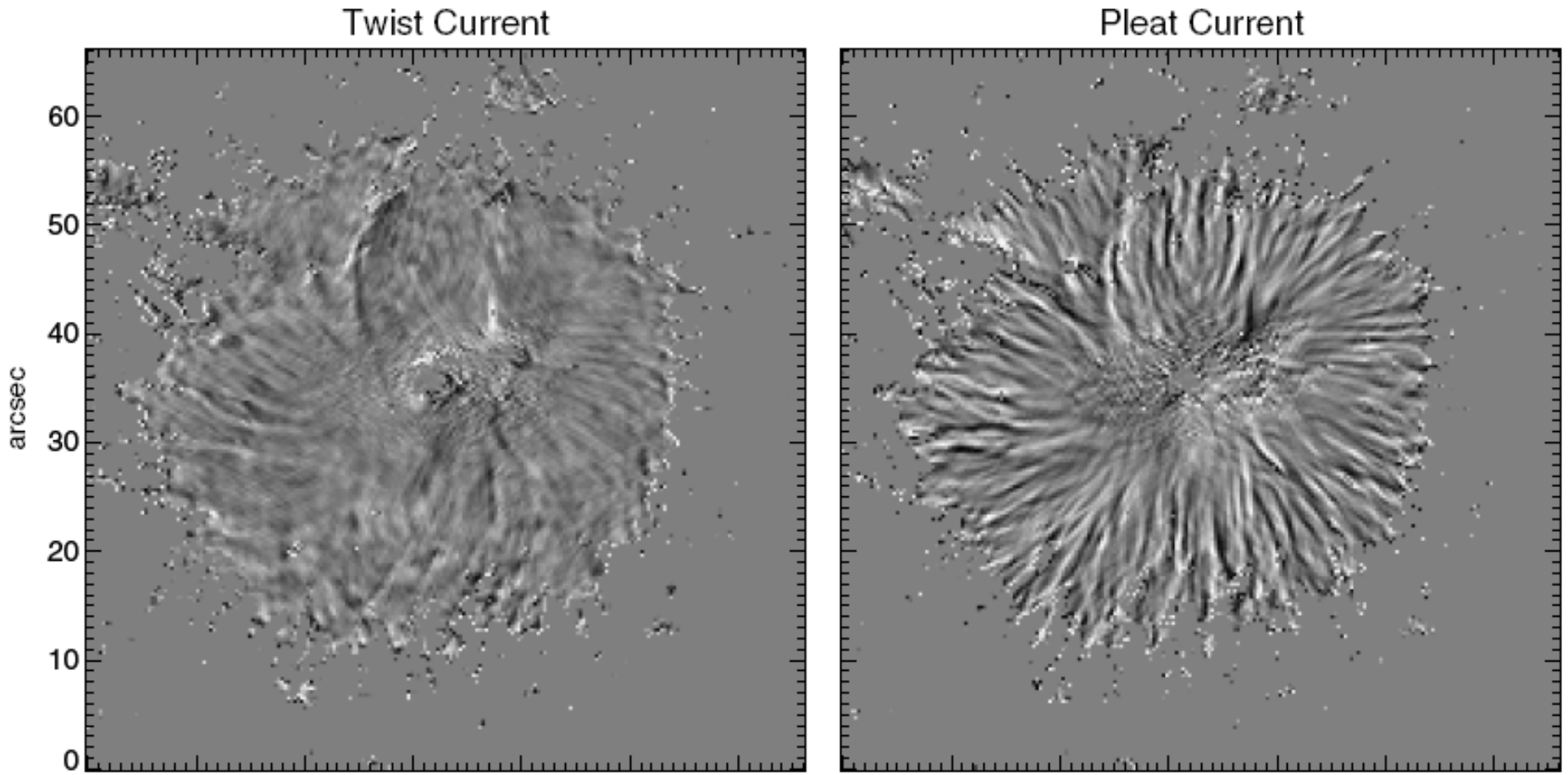
Twist Current
Pleat Current
arcsec
0
10
20
30
40
50
60

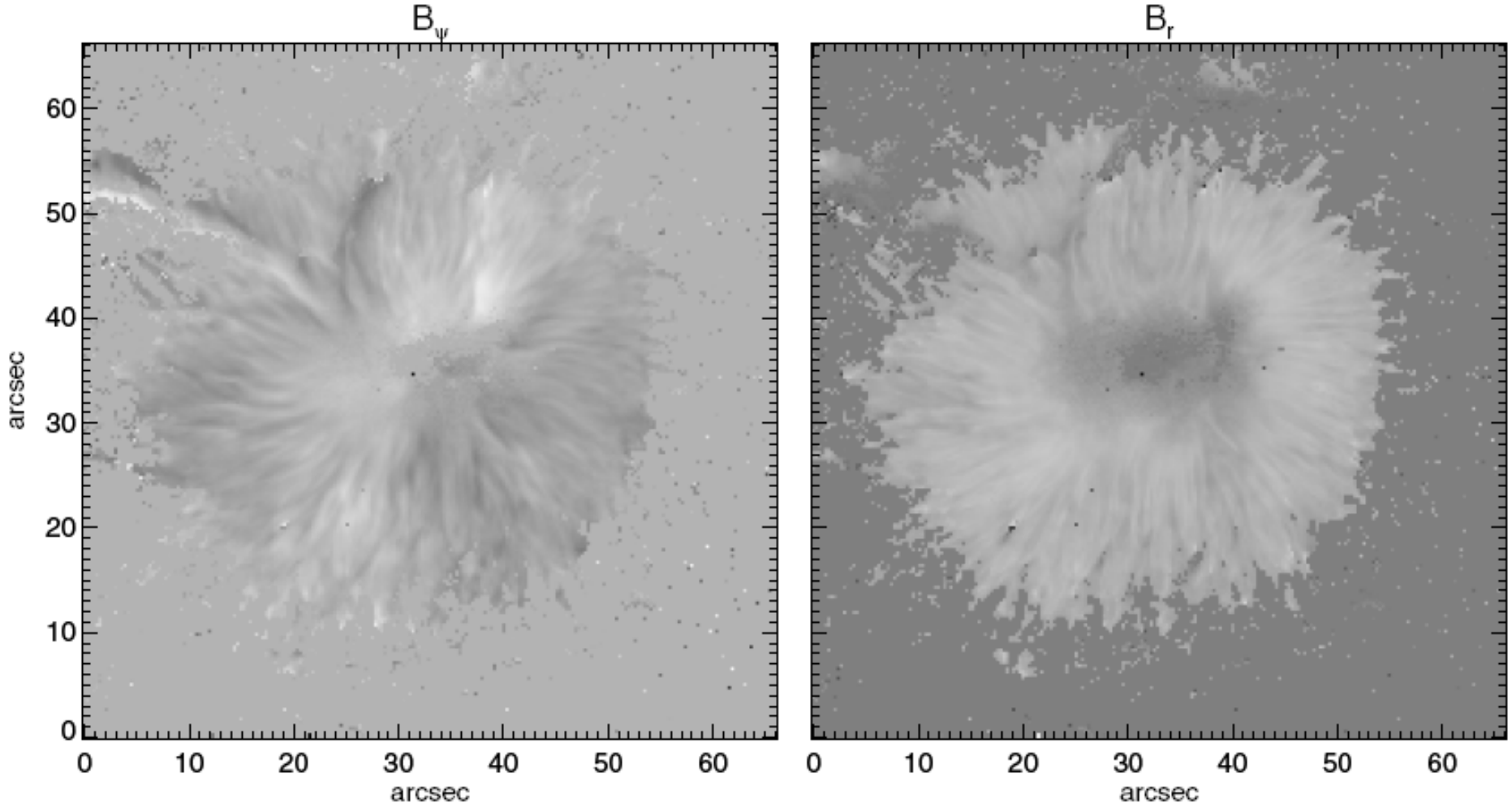
B_ψ
B_r
arcsec
arcsec
arcsec
0
10
20
30
40
50
60

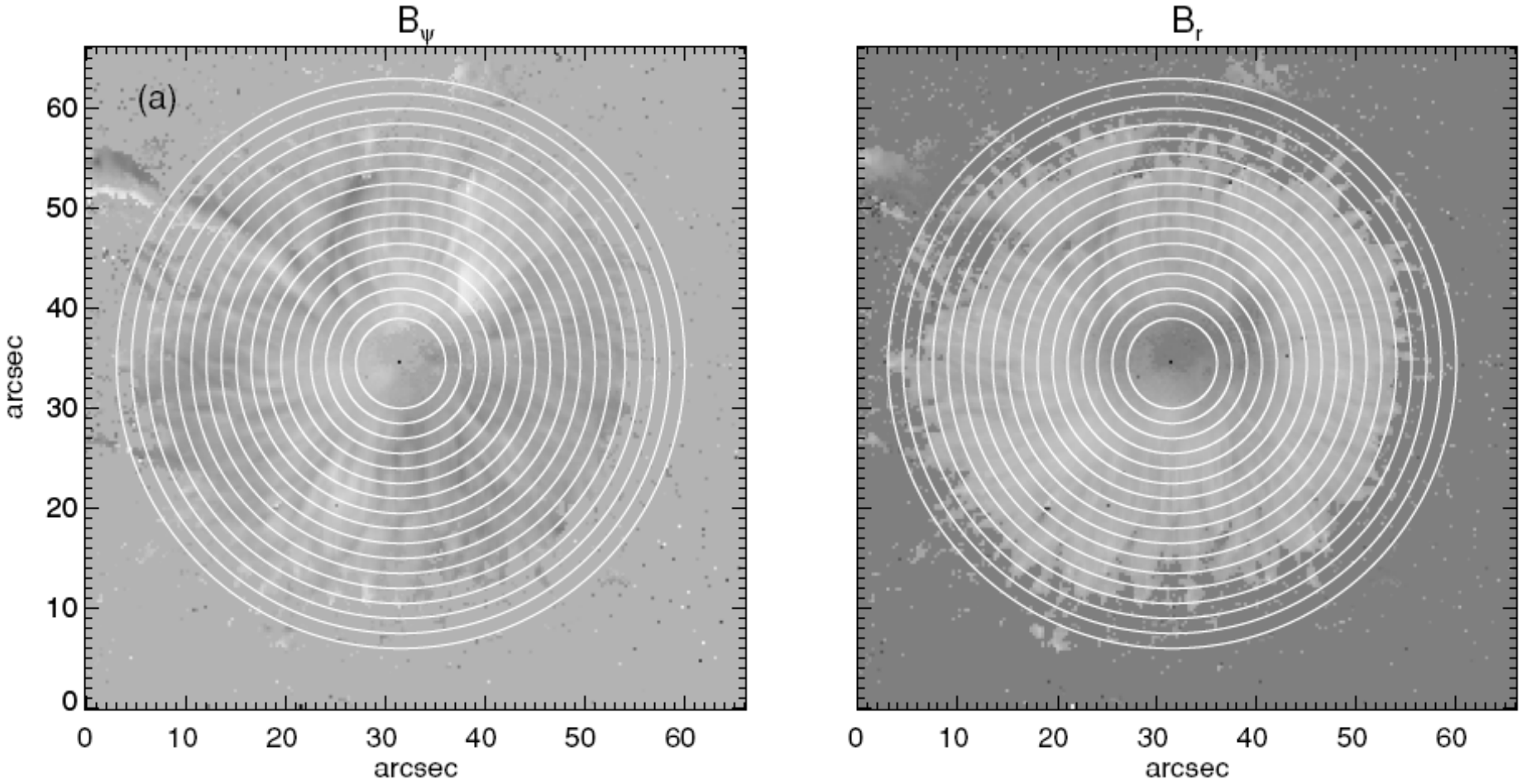
B_ψ
(a)
B_r
arcsec
arcsec
arcsec
0
10
20
30
40
50
60

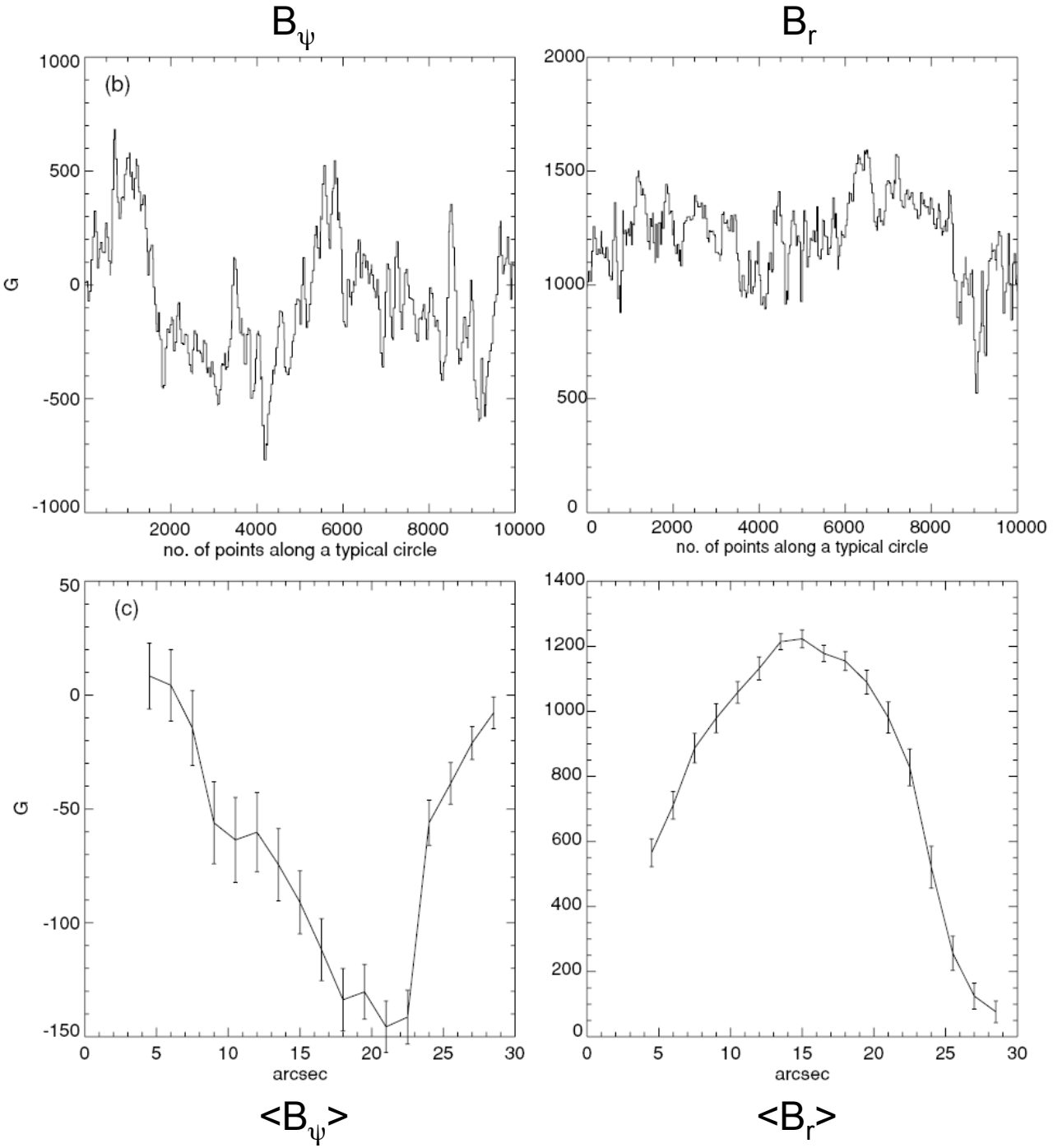
B_ψ
B_r
(b)
G
no. of points along a typical circle
no. of points along a typical circle
(c)
G
arcsec
arcsec
$<B_\psi>$
$<B_r>$

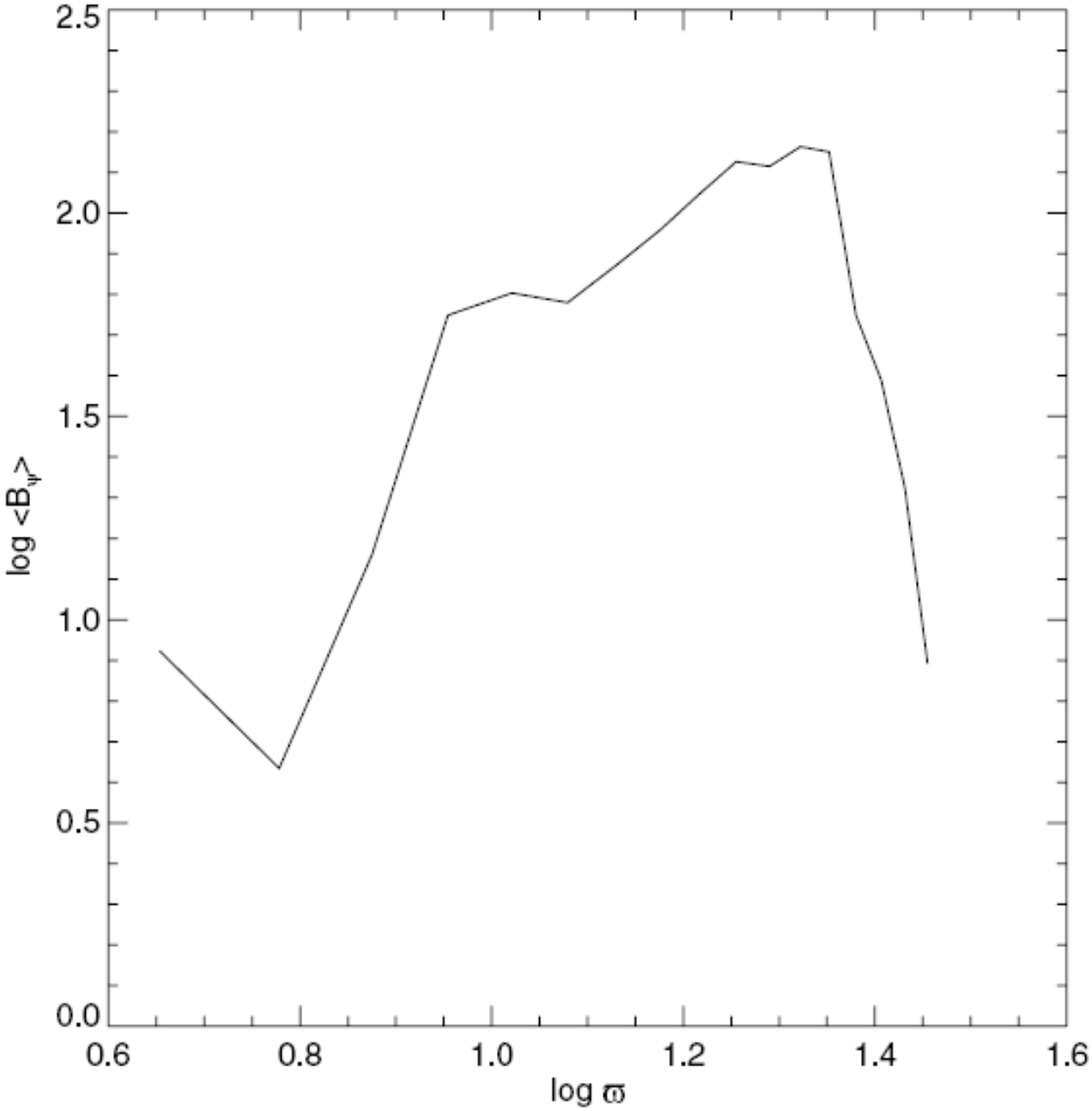
2.5
2.0
1.5
1.0
0.5
0.0
log <B_ψ>
0.6
0.8
1.0
1.2
1.4
1.6
log ϖ

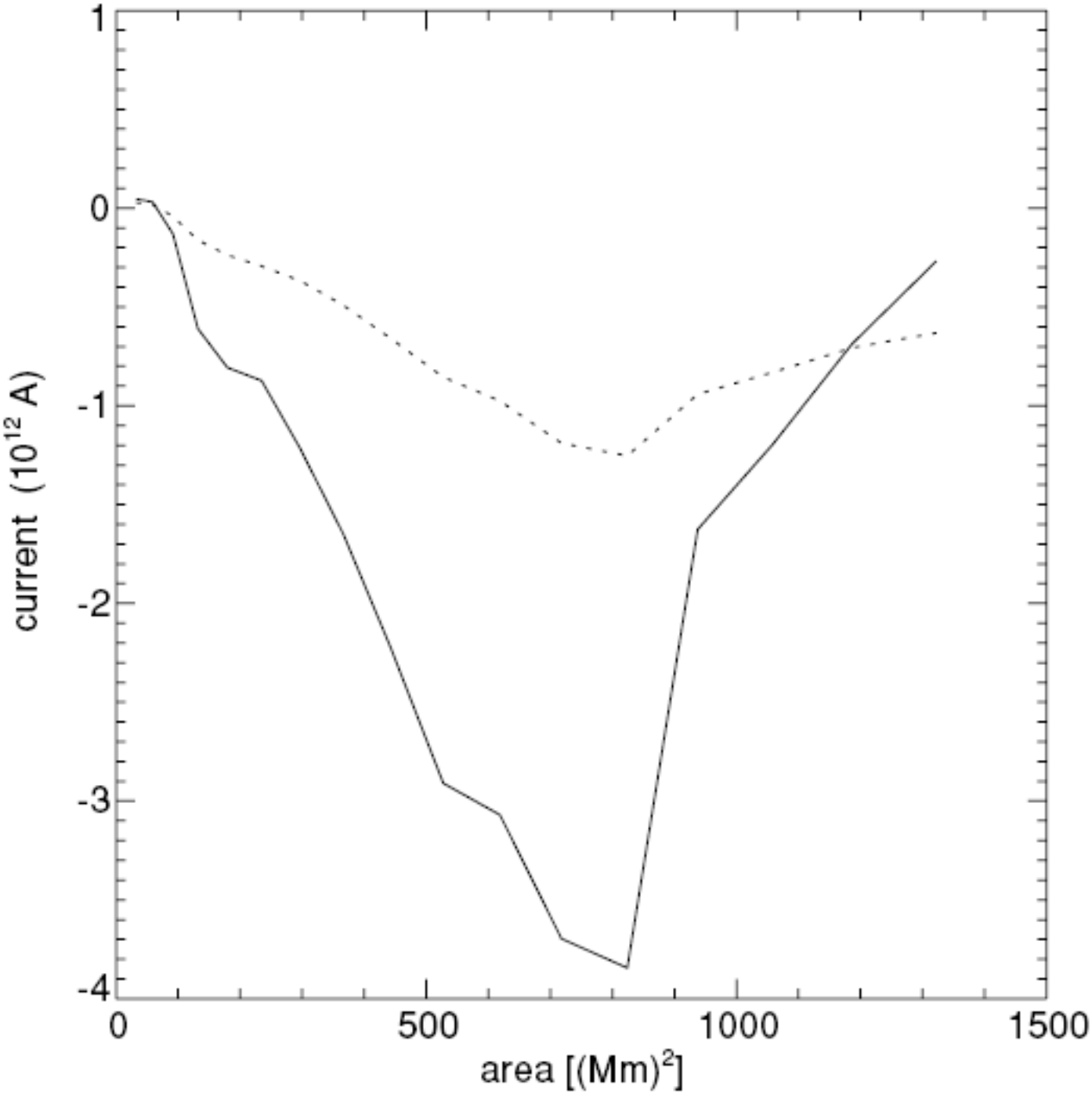
1
0
-1
-2
-3
-4
current (10^12 A)
0
500
1000
1500
area [(Mm)^2]

Table 1
List of the Active Regions Studied

AR No. (NOAA)	Date of Observation	Slope δ	Shear Angle (SSA; deg)	Twist Angle ($\tan^{-1}(B_\psi / B_r)$; deg)	Position	Hemispheric Helicity Rule
10969	2007 Aug 29	7.514	−4.488	−4.009	S05W33(t)	No
10966	2007 Aug 7	4.349	−5.120	−7.028	S06E20(t)	No
10963(−)	2007 Jul 12	4.366	−5.123	41.873[a]	S06E14(t)	No
10963(+)	2007 Jul 12	4.210	−4.495	−5.112	S06E14(t)	No
10961	2007 Jul 2	4.976	−4.973	29.451[a]	S10W16(t)	No
10960	2007 Jun 7	3.267	3.182	−24.012[a]	S07W03	Yes
10953	2007 Apr 29	8.249	−3.382	7.200[a]	S10E22(t)	No
10944	2007 Mar 3	2.407	−4.635	−5.130	S05W30(t)	No
10940	2007 Feb 1	2.281	−4.726	−7.950	S04W05	No
10933	2007 Jan 5	9.584	−2.283	−2.689	S04W01	No
10926	2006 Dec 3	2.750	−1.538	6.001[a]	S09W32(t)	No
10923	2006 Nov 10	3.175	0.785	−9.010[a]	S05W30(t)	Yes

Notes. The power index δ: the slope of decrease of B_ψ value, the twist angle, the signed shear angle (SSA), and other details of the sunspots are given. (t): transformed.

[a] Twist angle for irregular sunspots does not fit to a cylindrical assumption and therefore gives incorrect values.

DISCUSSION AND CONCLUSIONS

While it is difficult to detect fibrils using the Zeeman effect notwithstanding the superior resolution of SOT on *Hinode*, the stability and accuracy of the measurements have allowed us to detect the faster than $1/\varpi$ decline of the azimuthal component of the magnetic field, which in turn can be construed as evidence for the confinement of the sunspot field by the external plasma. The resulting pattern of curl **B** appears as a drop in net current at the sunspot boundary.

If this lack of net current turns out to be a general feature of sunspot magnetic fields in the photosphere, then measurement of helicity from a global average of the force-free parameter becomes suspect. On the other hand, sunspots are evidently twisted at photospheric levels, as seen from the non-vanishing average twist angle as well as the SSA (Table 1). Although the existence of a global twist in the absence of a net current is possible for a monolithic sunspot field (Baty 2000; Archontis et al. 2004; Fan & Gibson 2004; Aulanier et al. 2005), a fibril model of the sunspot field can accommodate a global twist even without a net current (Parker 1996).

The spatial pattern of current density in a sunspot (e.g., left panel of Figure 4) is really a manifestation of the deformation of the magnetic field ($\nabla \times \mathbf{B}$) by the forces applied by the plasma. The Lorentz force exerted by the field on the plasma produces an equal and opposite force by the plasma, thereby confining the field. Thus, our analysis actually shows the pattern of the forces exerted by the plasma on the field. The sharp decline of the azimuthal field with radial distance thus shows the confinement of the sunspot magnetic field by the radial gradient of the plasma pressure.

Parker (1996) also mentions the possibility of net currents in the corona, continuing down to the height where the first cleaving takes place. It would therefore be imperative to look for net currents at higher reaches of the solar atmosphere. This is very important because several theories of flares (Melrose 1995) and coronal mass ejection triggers (Forbes & Isenberg 1991; Kliem & T¨or¨ok 2006) rely heavily on the existence of net currents in the corona above the sunspots*.

Future large ground-based telescopes equipped with adaptive optics and multispectral line capabilities would go a long way in addressing these issues. In the meantime, direct measurement of the global twist of sunspots using parameters like the SSA should serve as proxies for estimating the net currents of active regions in the corona. The SSA will also be a better parameter to base a fresh look at the hemispheric rule in photospheric chirality.

* *Tibor T¨or¨ok however clarified that their simulated trigger does not need a net current*

Evolution of Net Current and Emergence of Bi-Directional Currents in the Flare Productive Active Region NOAA 10930

B. Ravindra[1]

[1]Indian Institute of Astrophysics, Koramangala, Bangalore 560 034, India

ravindra@iiap.res.in

and

P. Venkatakrishnan[2], Sanjiv Kumar Tiwari[2,3] and R. Bhattacharyya[2]

[2]Udaipur Solar Observatory, Physical Research Laboratory, Dewali, Bari Road, Udaipur-313 001, India

pvk@prl.res.in

tiwari@mps.mpg.de

ramit@prl.res.in

[3]Max-Planck-Institut für Sonnensystemforschung, Max-Planck-Str. 2, 37191 Katlenburg-Lindau, Germany

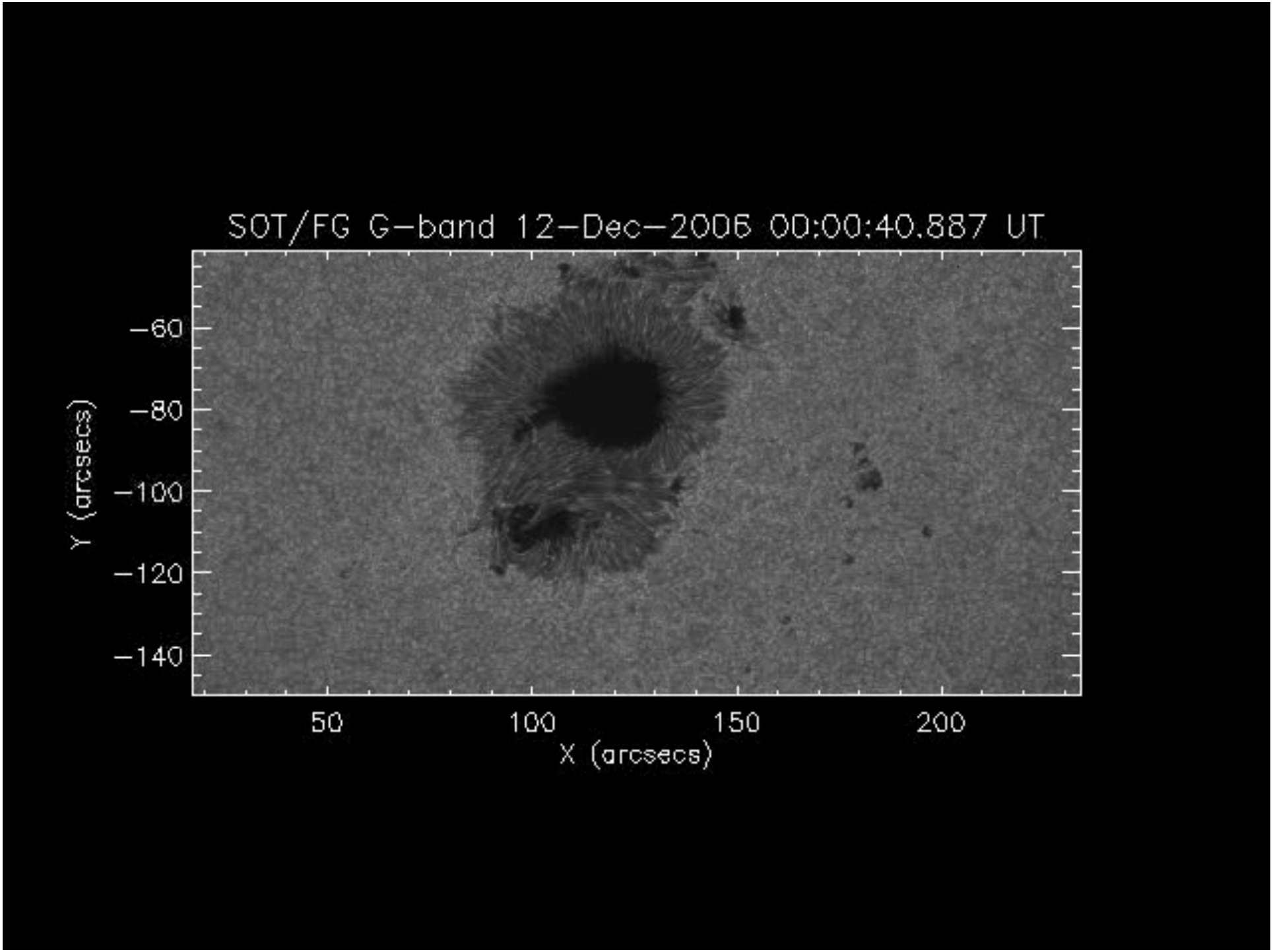
SOT/FG G-band 12-Dec-2006 00:00:40.887 UT
-60
-80
-100
-120
-140
Y (arcsecs)
50
100
150
200
X (arcsecs)

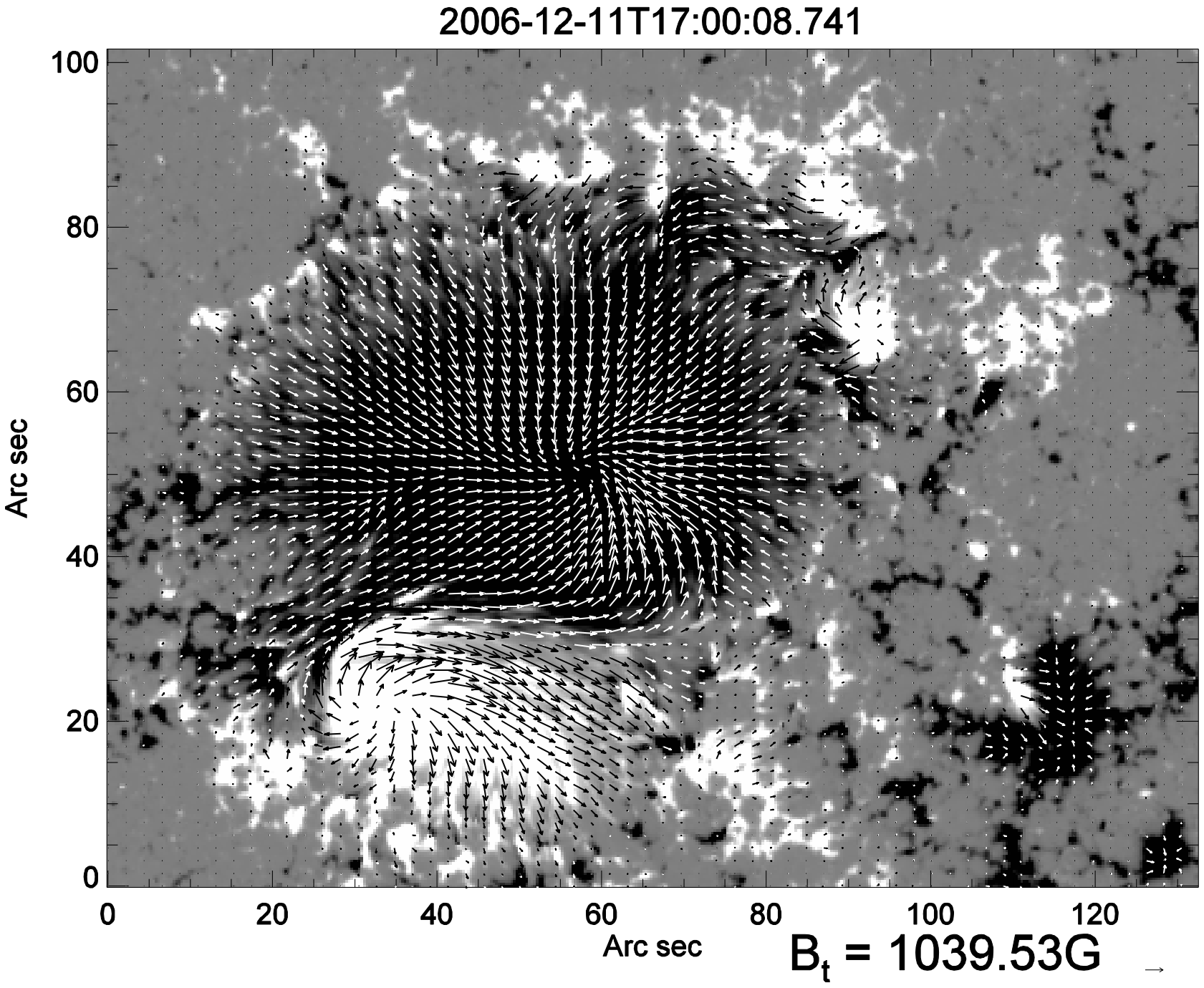
2006-12-11T17:00:08.741
100
80
60
40
20
0
Arc sec
0
20
40
60
80
100
120
Arc sec
B_t = 1039.53G

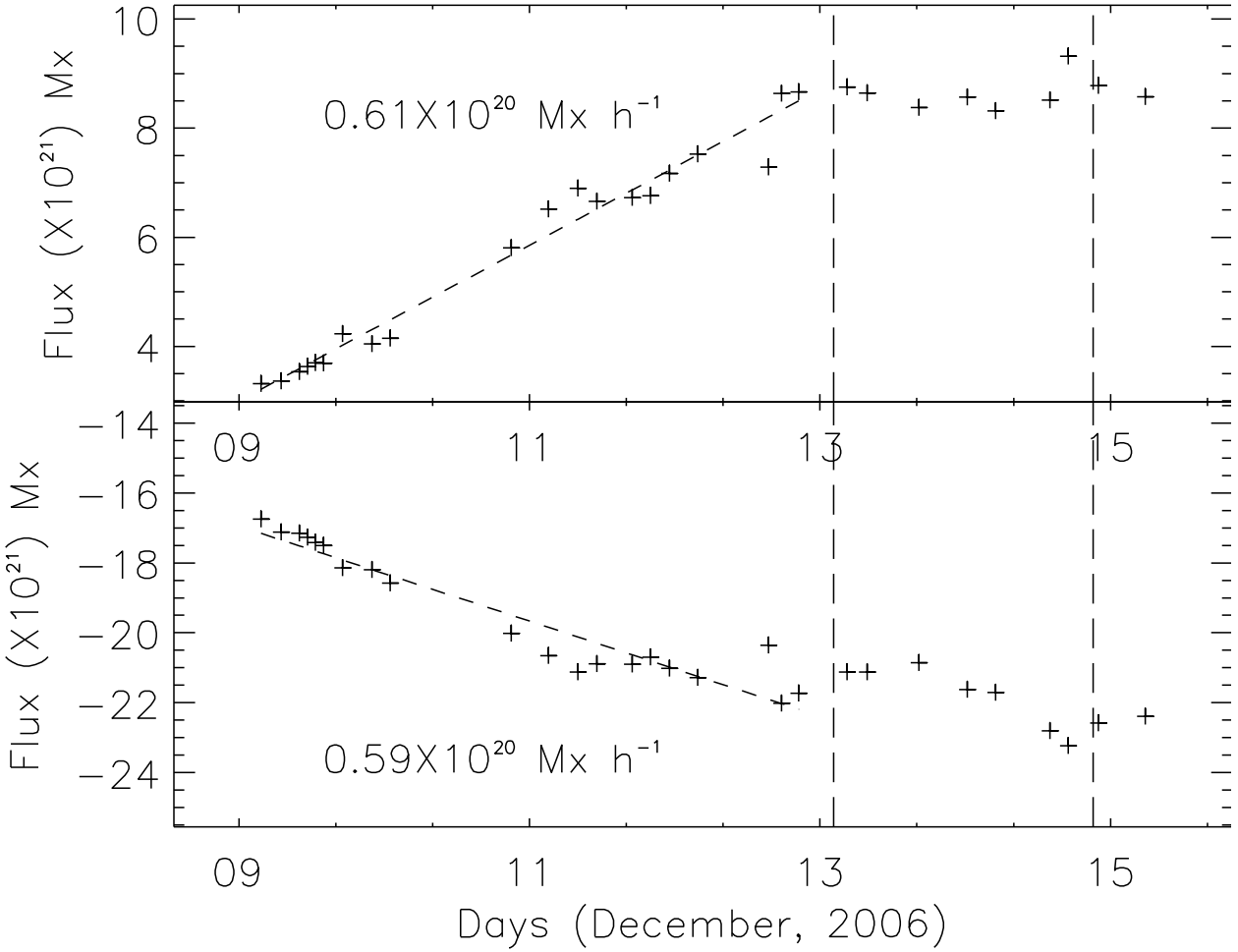
10
8
6
4
Flux (X10^21) Mx
0.61X10^20 Mx h^-1
09
11
13
15
−14
−16
−18
−20
−22
−24
Flux (X10^21) Mx
0.59X10^20 Mx h^-1
09
11
13
15
Days (December, 2006)

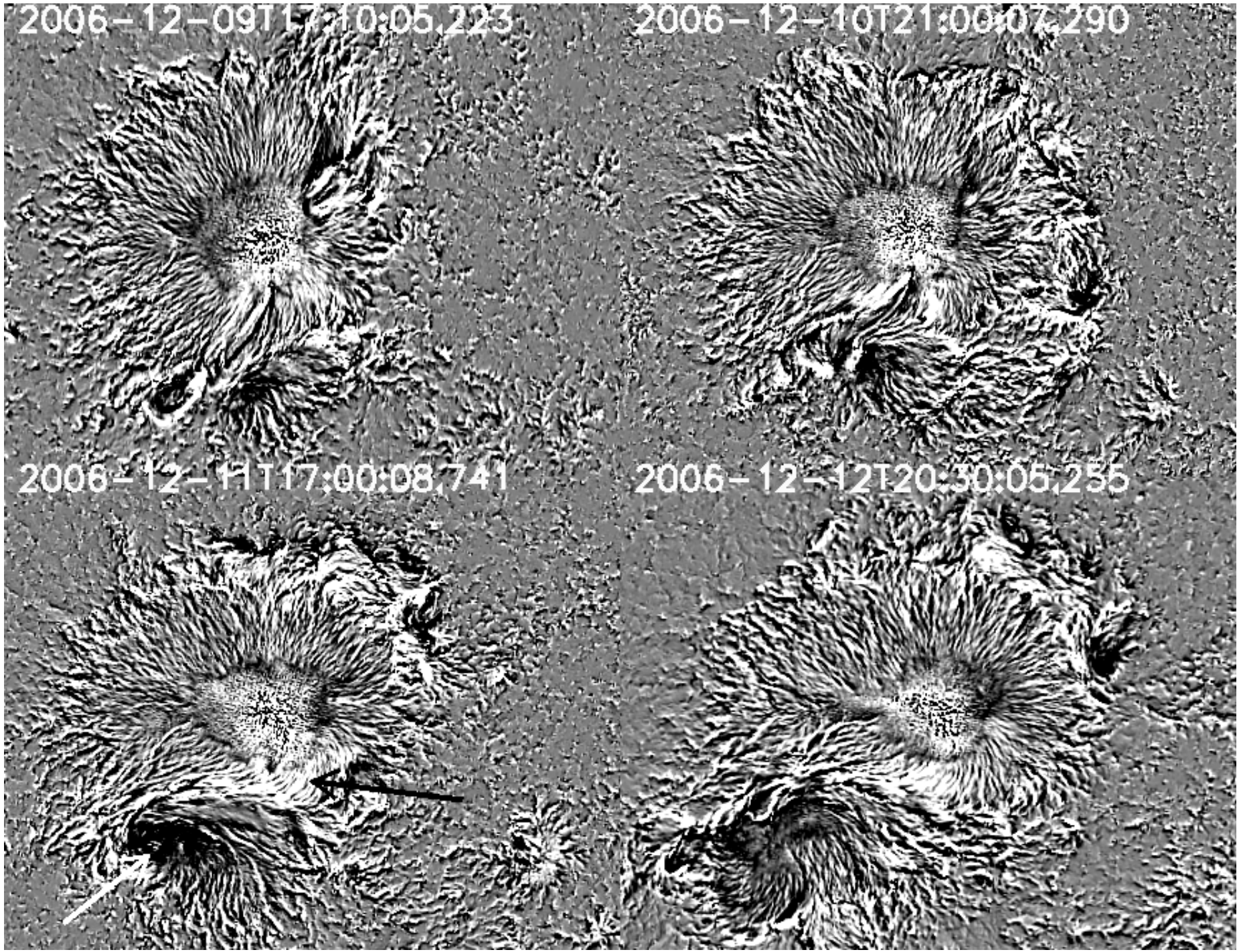
2006-12-09T17:10:05.223
2006-12-10T21:00:07.290
2006-12-11T17:00:08.741
2006-12-12T20:30:05.255

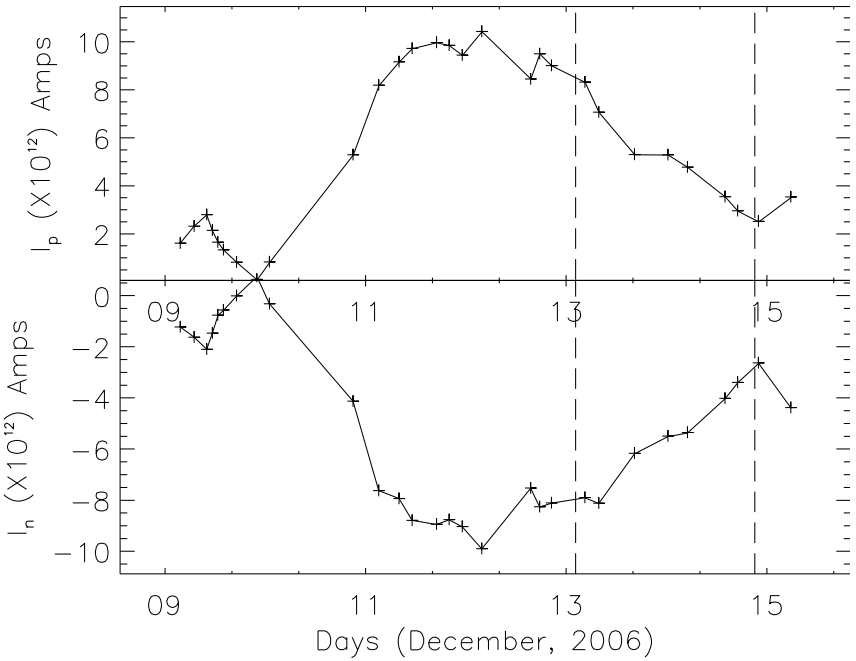
I_p ($X10^{12}$) Amps
I_n ($X10^{12}$) Amps
Days (December, 2006)

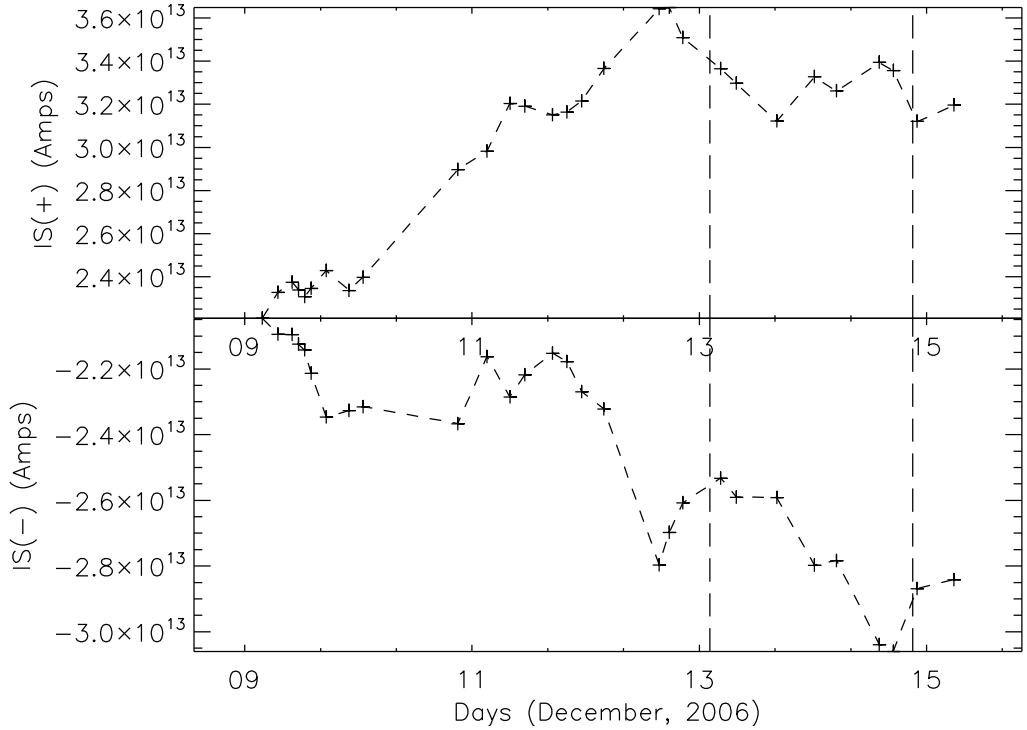
IS(+) (Amps)
IS(−) (Amps)
Days (December, 2006)

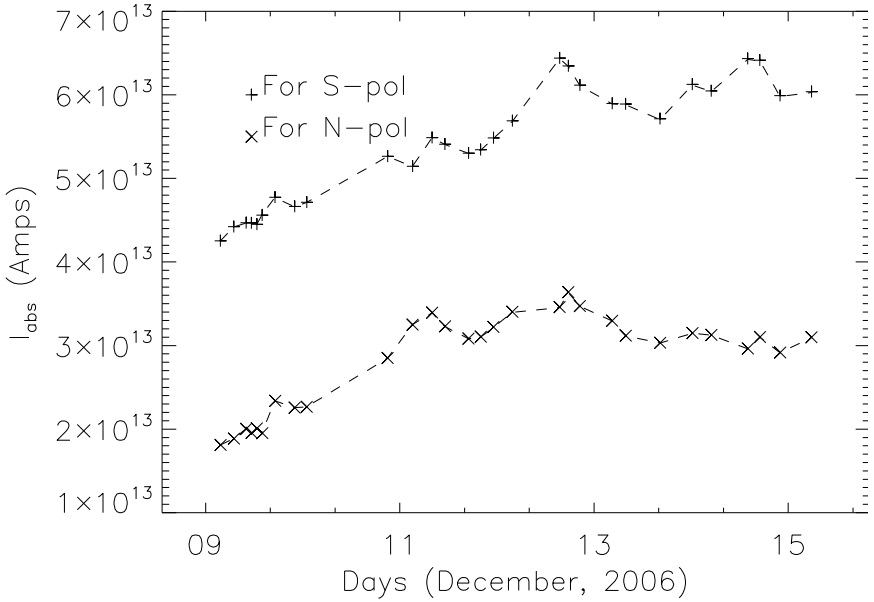
For S−pol
For N−pol
I_{abs} (Amps)
Days (December, 2006)

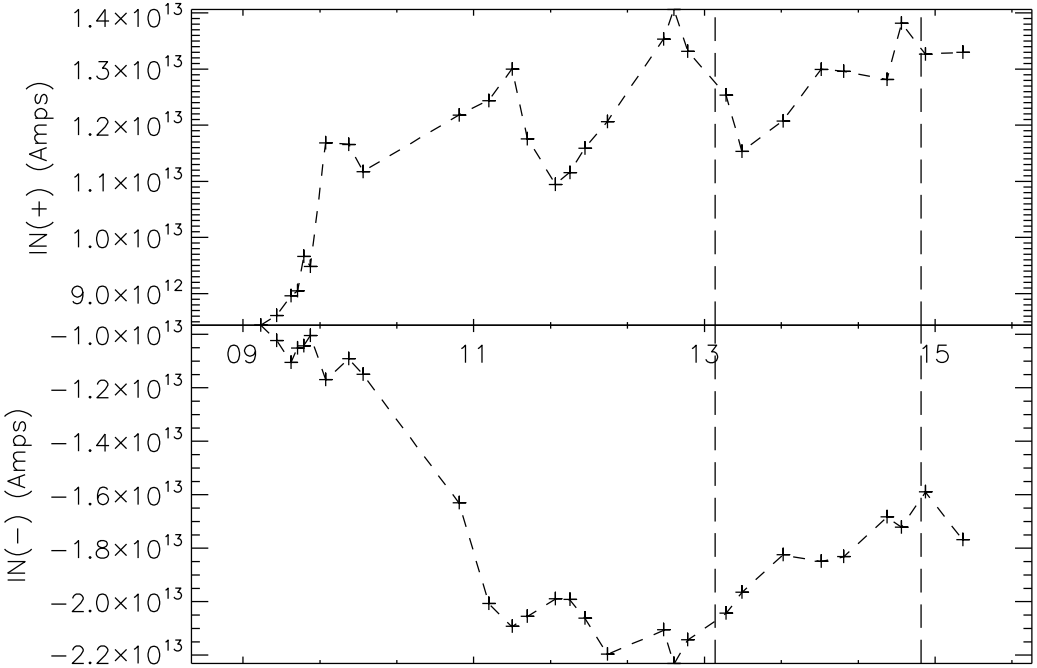
IN(+) (Amps)
IN(−) (Amps)

$$\nabla \times \mathbf{B}_o = \alpha_o \mathbf{B}_o$$
$$\nabla \times \mathbf{B}_n = \alpha_n \mathbf{B}_n \ ,$$

$$\mathbf{B} = \mathbf{B}_o + \mathbf{B}_n \ .$$

$$\mathbf{J} = \frac{1}{\mu} \left(\alpha_o \mathbf{B}_o + \alpha_n \mathbf{B}_n \right) \ .$$

$$\mathbf{J} \times \mathbf{B} = \frac{1}{\mu} (\alpha_o - \alpha_n) \mathbf{B}_o \times \mathbf{B}_n \ .$$

Opposite current can introduce Lorentz force

When opposite current ceases to emerge, coronal field will settle to a new force free equilibrium

MAGNETIC NON-POTENTIALITY OF SOLAR ACTIVE REGIONS AND PEAK X-RAY FLUX OF THE ASSOCIATED FLARES

SANJIV KUMAR TIWARI, P. VENKATAKRISHNAN, AND SANJAY GOSAIN

THE ASTROPHYSICAL JOURNAL, 721:622–629, 2010 September 20

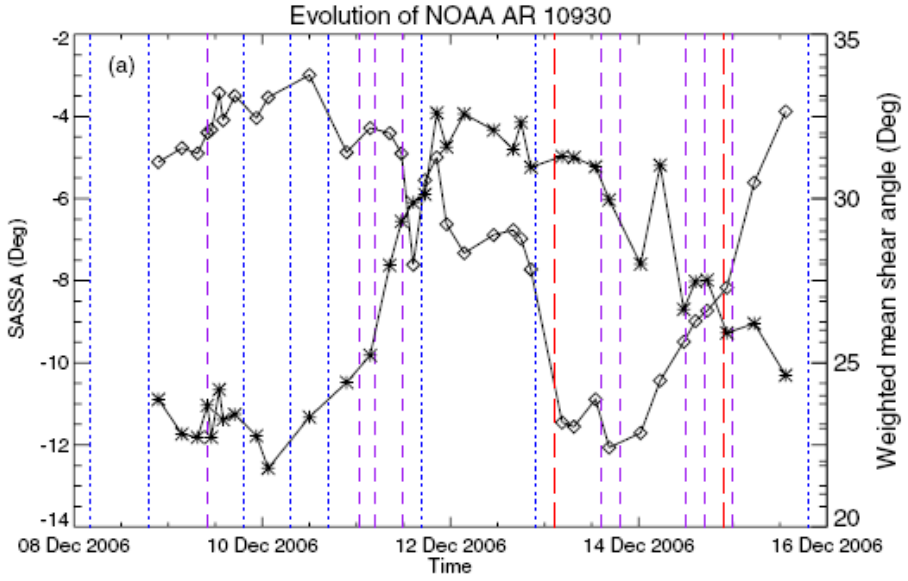

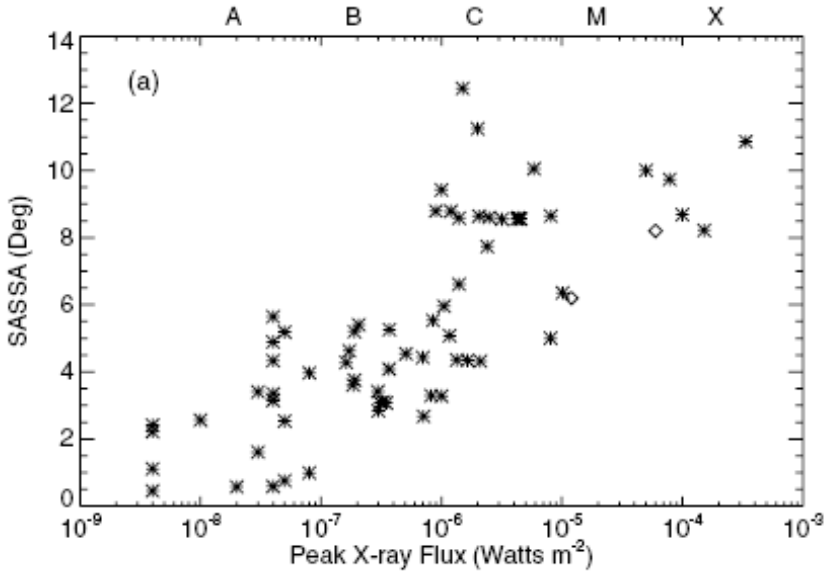

TEMPORAL CHANGES IN SUNSPOT UMBRAL MAGNETIC FIELDS AND TEMPERATURES

M. J. Penn and W. Livingston

The Astrophysical Journal, 649: L45–L48, 2006 September 20

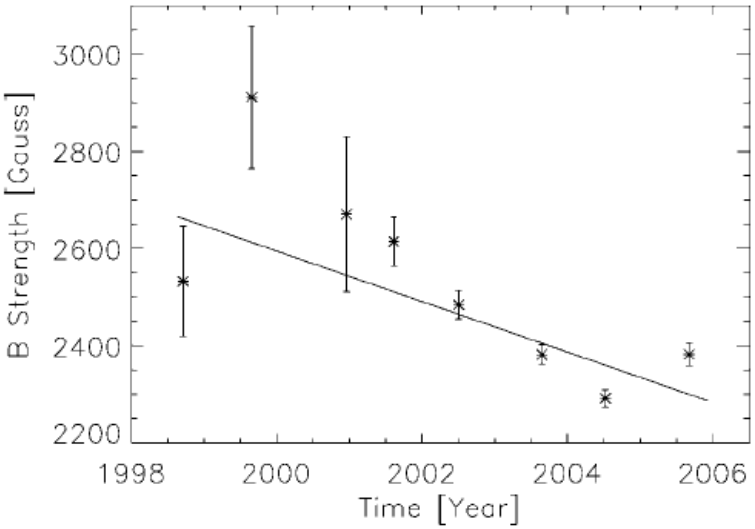

Fig. 2.—Magnetic field computed from the Zeeman splitting of the Fe I 1564.8 nm line, shown for umbral spectra observed from 1998 through 2005. While there is a large variation between different sunspots, nonparametric tests confirm that the data show a highly significant trend. The mean values for each calendar year are shown as data points, and the error bars show the standard error of the mean. The best-fit linear function (fit to the original 906 data points) reveals a decrease in the average magnetic field strength of 52 G yr^{-1}.

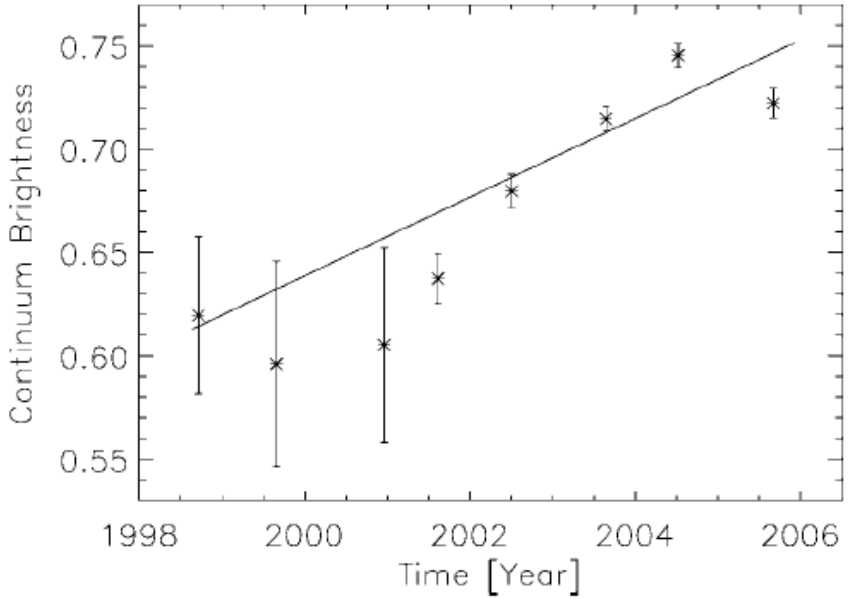

Fig. 3.—Continuum intensity of the umbral spectra, normalized to the intensity of the nearby quiet Sun, shown from 1998 through 2005. The points, error bars, and linear fit are computed as in Fig. 2. A linear fit to the data shows a temperature increase of about 73 K yr^{-1}.

A&A 465, 291–304 (2007)

I. Dependence of brightness on sunspot size and cycle phase

S. K. Mathew[1,2], V. Martínez Pillet[3], S. K. Solanki[1], and N. A. Krivova[1]

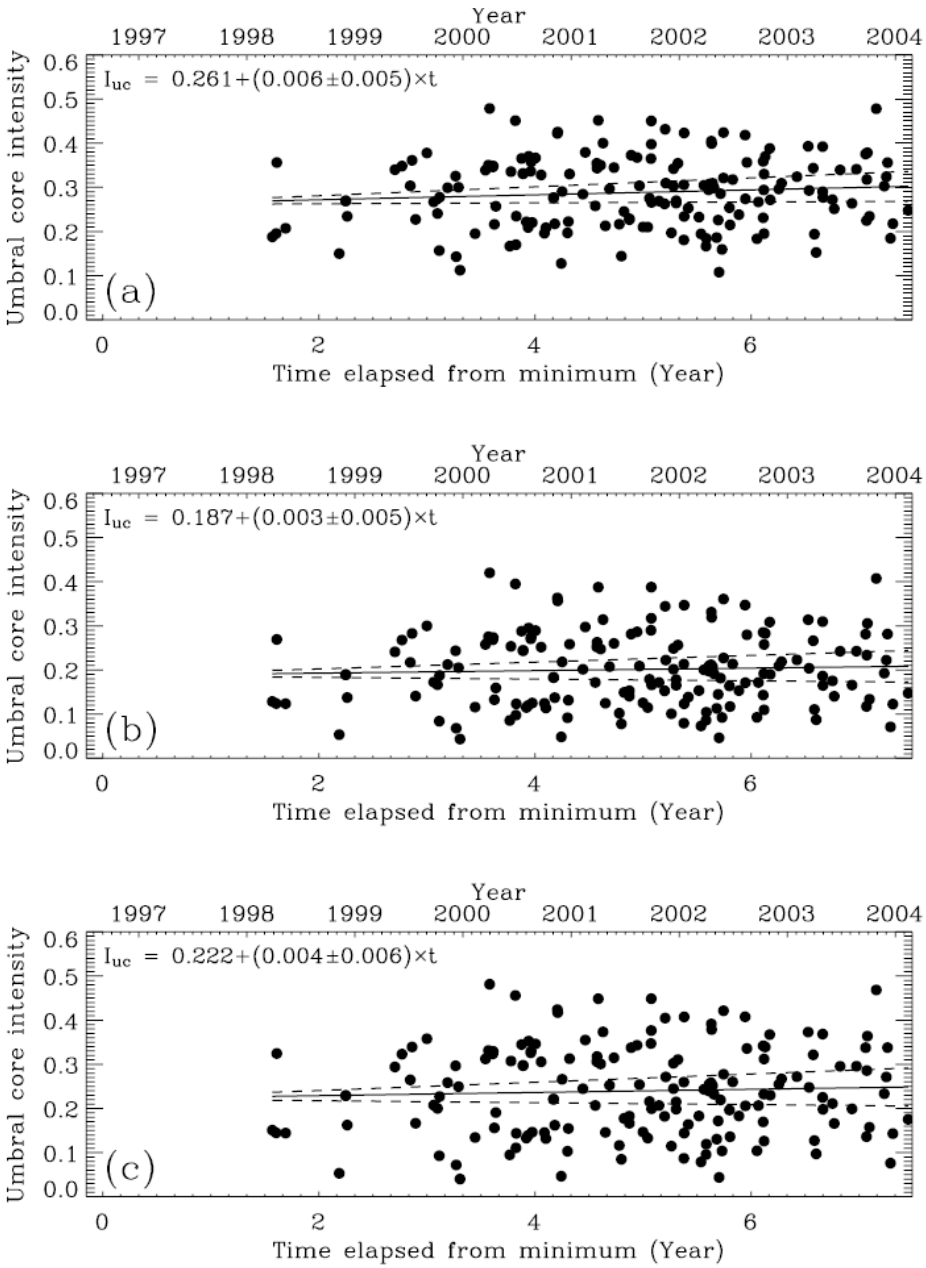

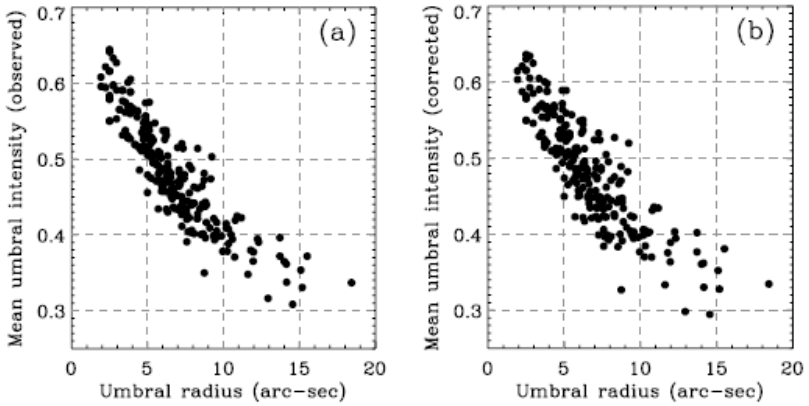

Fig. 11. Mean umbral intensity versus umbral radius, **a)** observed and, **b)** corrected for stray light and the influence of the Ni I line. Here sunspots with umbral radius less than 5 arcsec and greater than 15 arcsec are also included.

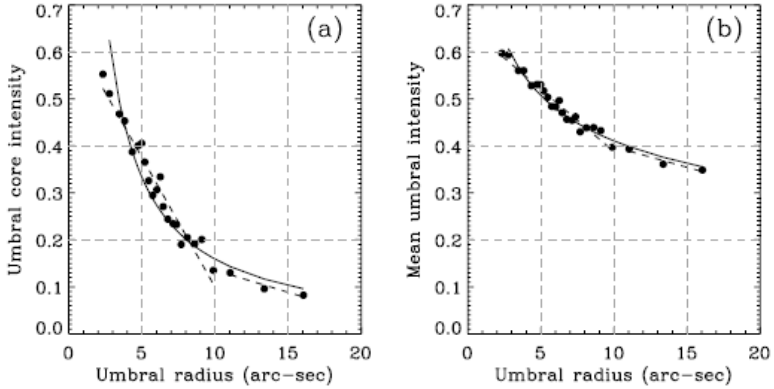

Fig. 12. Power law fit (solid line) and double linear fit (dash lines) to the **a)** umbral core intensity and, **b)** mean umbral intensity. Here the filled circles represent bins of 10 spots each.

Fig. 14. Umbral core intensity versus solar cycle, **a)** observed, **b)** corrected for stray light, and **c)** corrected for stray light and the influence of Ni I line. The intensities are plotted for all spots with umbral radii between 5 arcsec and 15 arcsec. The solid line shows the linear regression and the dashed lines represent the $\pm 1\sigma$ deviation, due to the uncertainty in the regression gradient. The best linear fit is given in the upper left corner.

Long-term Evolution of Sunspot Magnetic Fields

Matthew Penn, William Livingston

To appear in IAU Symposium No. 273

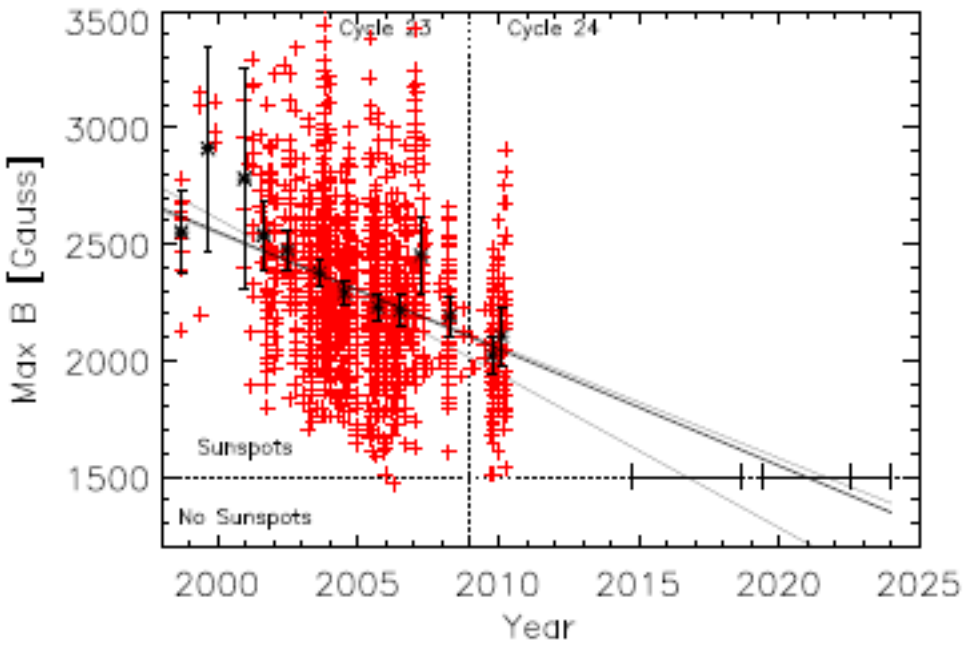

Fig. 1.— Measurements of the total magnetic field strength at the darkest location in umbrae and pores as a function of time. The crosses show the individual measurements, the asterisks show annual bins. Three linear fits are shown: the bottom fit line fits data from 1998-2006 as done in our 2006 paper. The top line fits all the data from Cycle 23, and the middle line fits all of the data.

- Minimum Field Strength of sunspot is related to pressure equipartition
- Higher Fields can be produced in force free equilibria
- Maximum field strength is related to conditions in the deeper layers: Strength of vortices
- Helioseismology does place sunspots at vortex junctions
- Umbral brightness is related to amount of field free plasma within a pixel
- Larger fields, being force free, are not confined by field free plasma and hence will appear darker

Conclusions

- Plasma confines sunspot fields into small structures thereby requiring zero net current
- Measured currents do not show up the surface currents of the structured field, but future large telescopes can detect these
- Measured net current evolves and is directly related to magnetic shear at polarity inversion lines
- Emergence of opposite currents leads to Lorentz force and possibly to eruptions
- Magnetic parameters like average shear and total current on the global scale of sunspots do relate to eruptions inspite of large fluctuations within the spot: Are sunspots self-organized coherent structures?
- Telescopes like MAST will track the height and time variation of net current thereby giving better extrapolation of coronal currents
- NLST, equipped with IR capabilities, should give an explanation for correlation between umbral field and brightness


THANKS

SUPERSONIC DOWNFLOWS AT THE UMBRA-PENUMBRA BOUNDARY OF SUNSPOTS

- Presence of supersonic downflows at or close to the umbra-penumbra boundary, sizes > 2 arcsec^2 usually encompassing bright penumbral filaments on center side of the spots
- Lifetimes of these downflows > 6 hr
- Strong, long-lived chromospheric brightenings observed in neighborhood of downflows.
- Slingshot Reconnection mechanism Ryutova et al. (2008a) may be responsible for the supersonic downflows, however the process is probably different from that driving microjets.

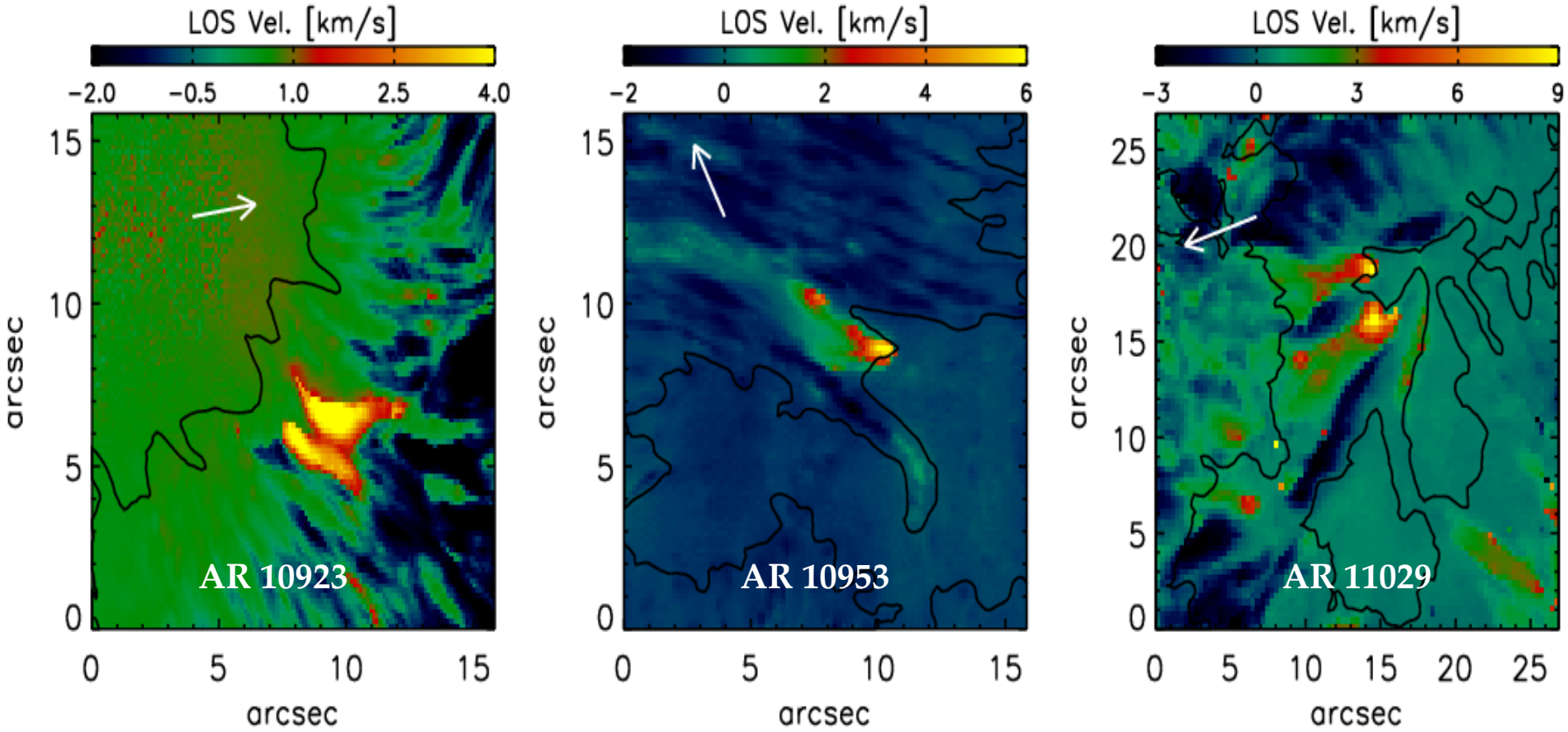

LOS velocities derived from the SIR inversion. Positive velocities indicate downflows. The maps have been scaled individually. The white arrow points to disc centre.

--- Rohan and Venkatakrishnan

On the Absence of Photospheric Net Currents in Vector Magnetograms of Sunspots Obtained From Hinode (SOT/SP)

P. Venkatakrishnan, and Sanjiv Kumar Tiwari

Astrophys. J., Letters, 2009, 706, L114-119

We studied 14 sunspots based on the data sets taken from Hinode (SOT/SP)

The global current is found absent or very small in all the sunspots in accordance with the theory of Parker (1996).

The existence of global twist for sunspots in absence of global current is an evidence for fibril-bundle structure of sunspots.

"Twist Angle" and Signed Shear Angle for circular sunspots are found equal as expected but for irregular sunspots they are not. Thus SSA is the best measure of sunspot twist at observed heights irrespective of shape of sunspots.

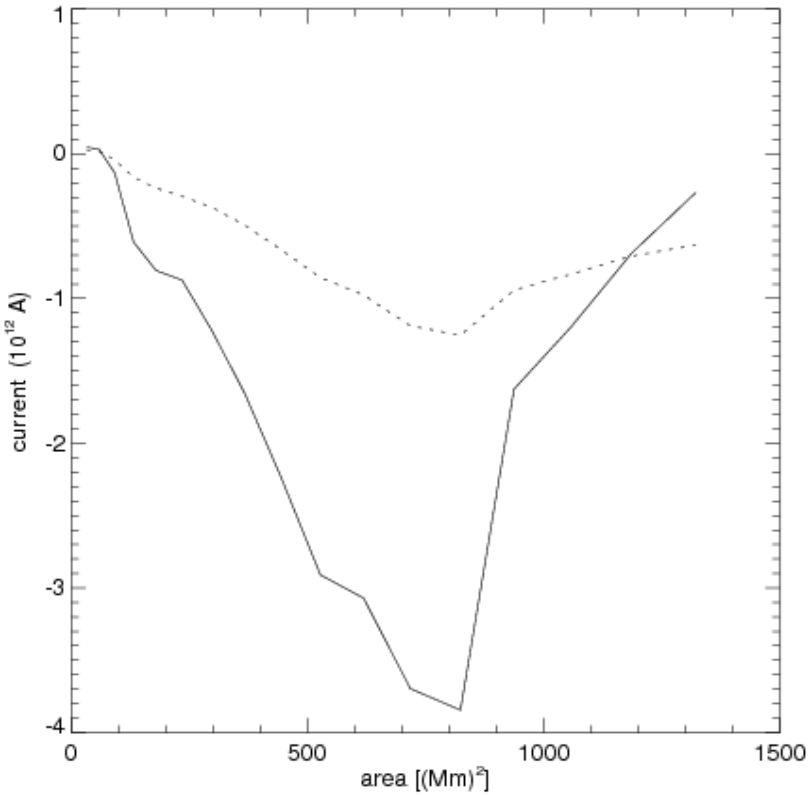

Net current variation with increasing area - solid line shows the results of our calculations (Venkatakrishnan and Tiwari, 2009), dashed line the results from the derivative method. The net current reduces very fast after a peak and almost vanishes for complete sunspot. On the other hand the net current computed from the derivative method shows a shallow behaviour.

Magnetic Tension of Sunspot Fine Structures

P. Venkatakrishnan, and Sanjiv Kumar Tiwari

A&A Letters, 2010, 516, L5

- Tension force is one component of the Lorentz force which balances the gradient of magnetic pressure in force-free configurations.

- We employ the tension term of the Lorentz force to clarify the structure of sunspot features like penumbral filaments, umbral light bridges and outer penumbral fine structures.

We find highly inhomogeneous distribution of tension with both positive and negative signs in various features of the sunspots.

Upward directed tension at the PIL of AR 10930 seems to be related to flux emergence.

The magnitude of the tension force is comparable or greater than the force of gravity in some places, implying a force-free configuration for these sunspot features.

The study of magnetic tension in various types of sunspot fine structures promises to yield new and exciting information on the equilibrium and dynamics of these structures.

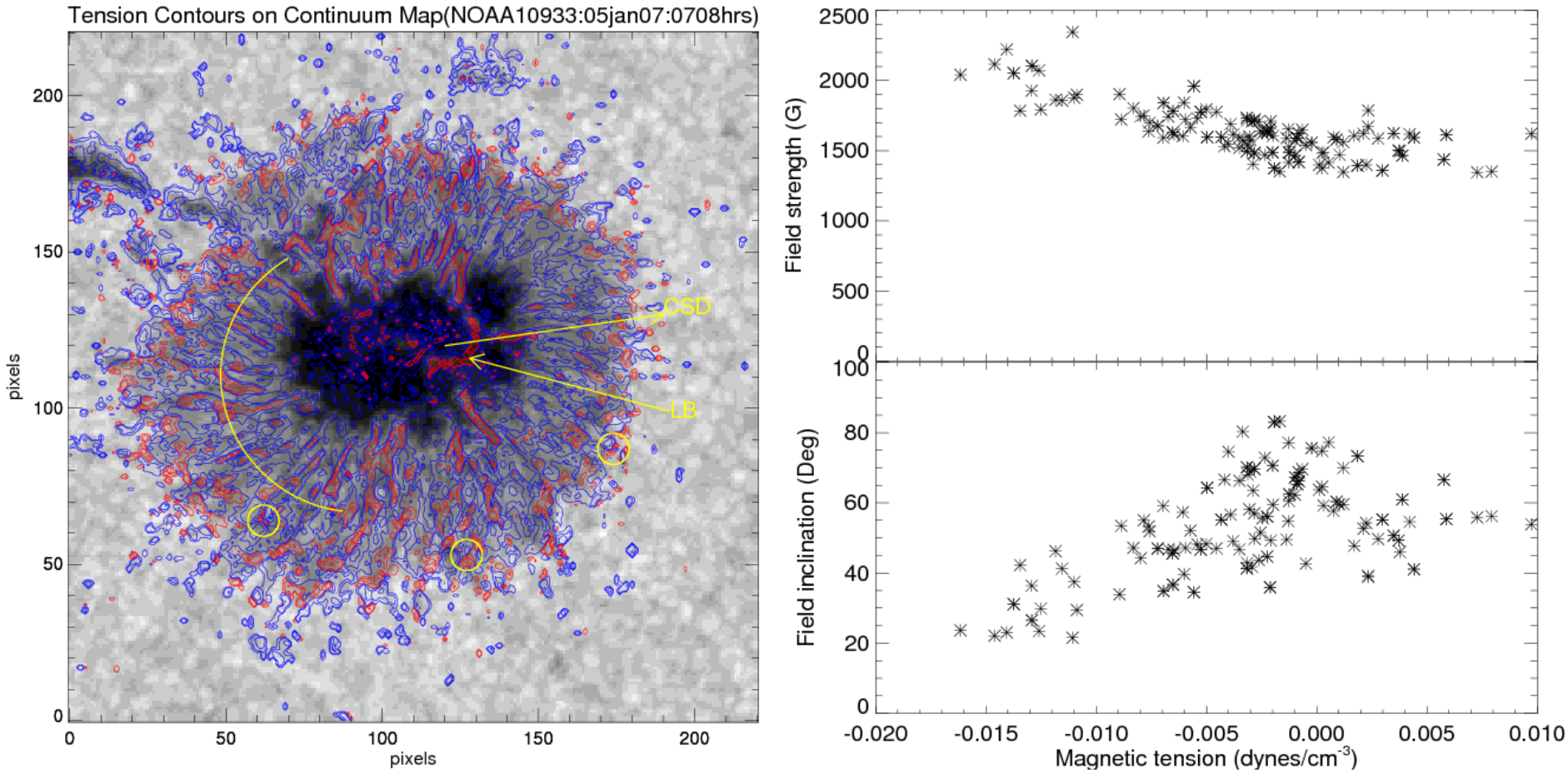

Contours of tension forces overlaid on the continuum map of NOAA AR 10933 (S04E05). Blue (red) colors show negative (positive)contours of ±1.2, ±4, ±12 millidynes/cm^{-3}. The position of a light bridge(LB) and three examples of bipolar sea serpent regions are shown by an arrow and by circles, respectively. An arc is shown for which the scatter plots of tension, fieldstrength, and inclination are shown in right panel.The heliocentric angle is θ = 8 deg, and an arrow points towards thecenter of the solar disk (CSD).

Evolution of Twist-shear and Dip-shear in sunspot during flare

To Appear in ApJ Letters)

Sanjay Gosain and P. Venkatakrishnan

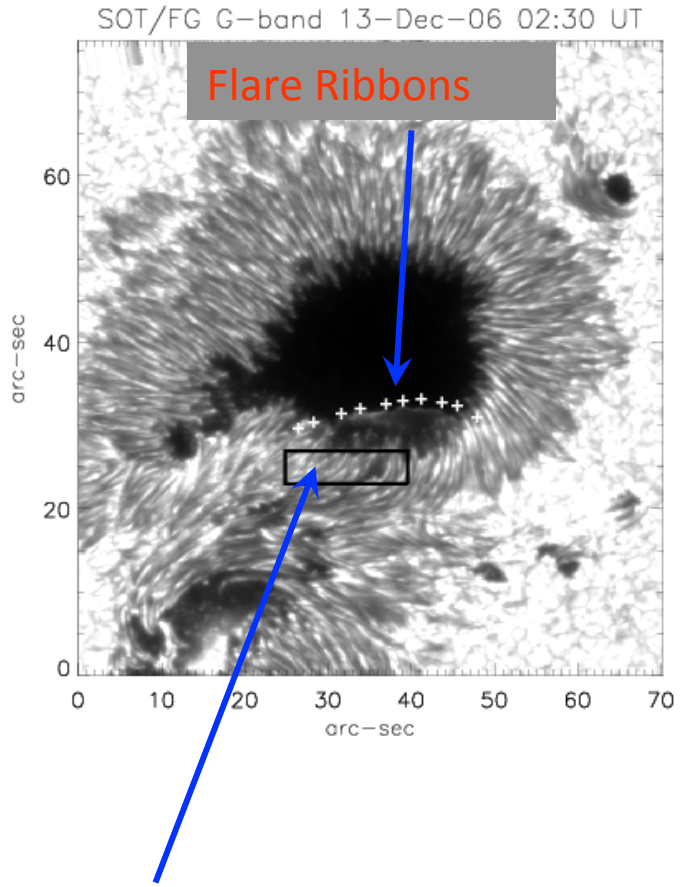

- Dip-shear and Twist-shear monitored in this box
- Flare ribbons sweep past this box during flare.

Main Results :

the *penumbral area* close to the *flaring site* shows *high value of twist-shear and dip-shear* as *compared to other parts* of penumbra,

(ii) *after the flare the value of dip-shear drops* in this region while the *twist-shear in this region tends to increase*,

(iii) the *dip-shear and twist-shear are correlated* such that pixels with large twist- shear also tend to exhibit large dip-shear, and

(iv) the *correlation* between the *twist-shear and dip-shear* is *tighter after the flare*.

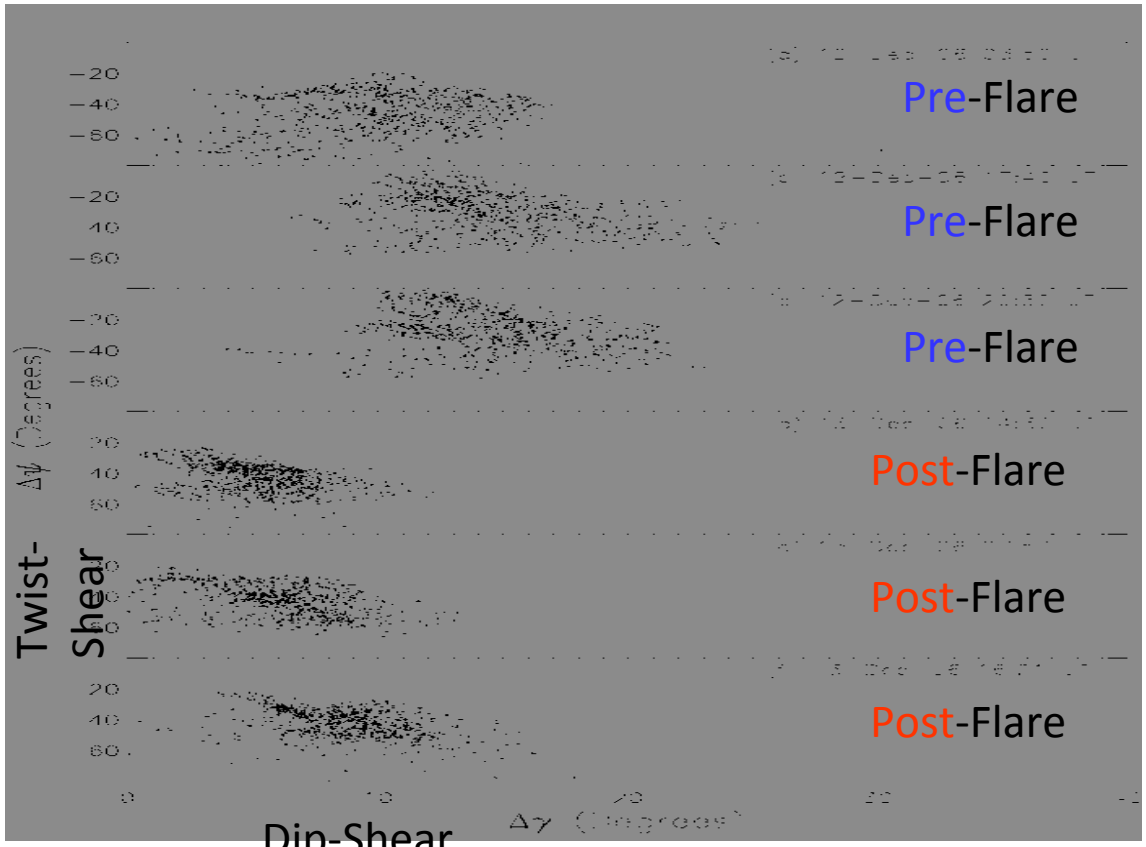

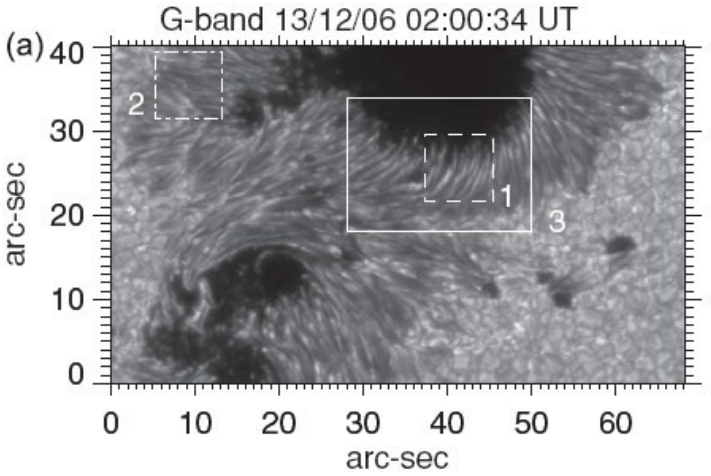
G-band 13/12/06 02:00:34 UT
(a)
2
1
3
arc-sec
arc-sec

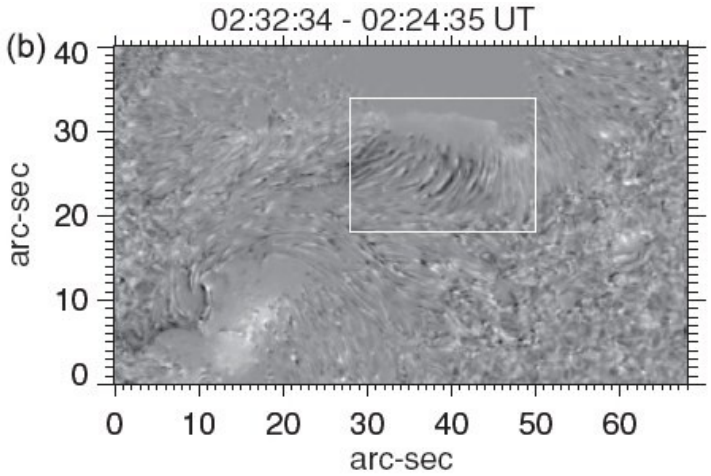
02:32:34 - 02:24:35 UT
(b)
arc-sec
arc-sec

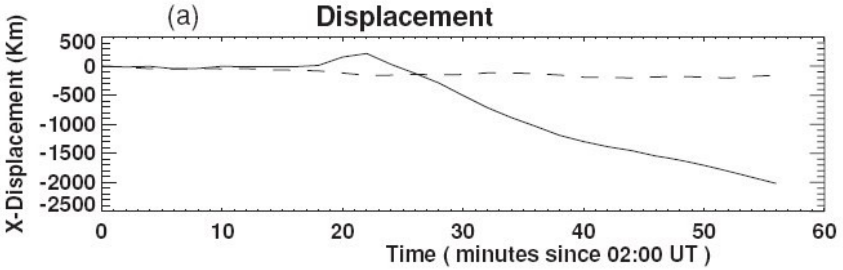
(a)
Displacement
X-Displacement (Km)
Time (minutes since 02:00 UT)

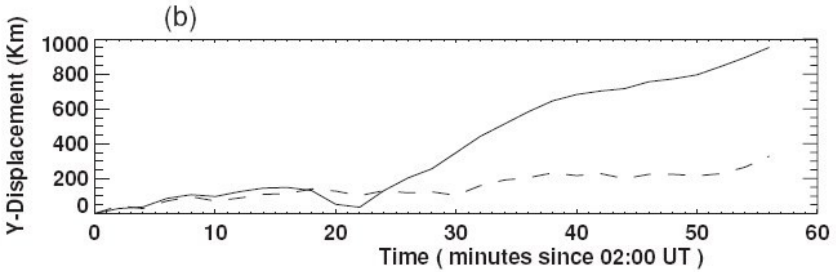
(b)
Y-Displacement (Km)
Time (minutes since 02:00 UT)

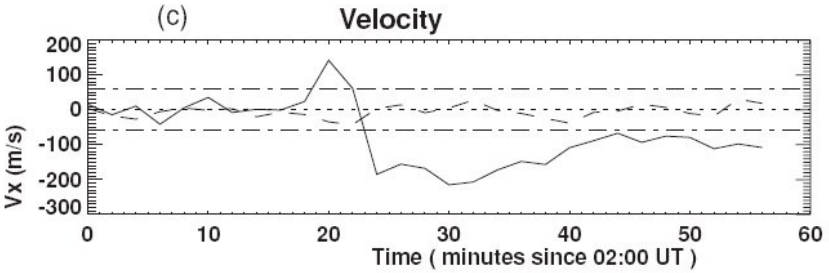
(c)
Velocity
Vx (m/s)
Time (minutes since 02:00 UT)

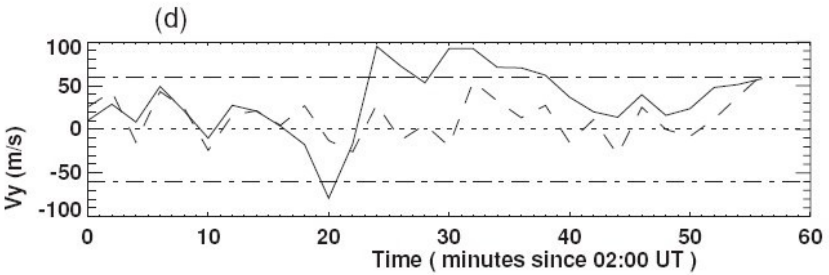
(d)
Vy (m/s)
Time (minutes since 02:00 UT)

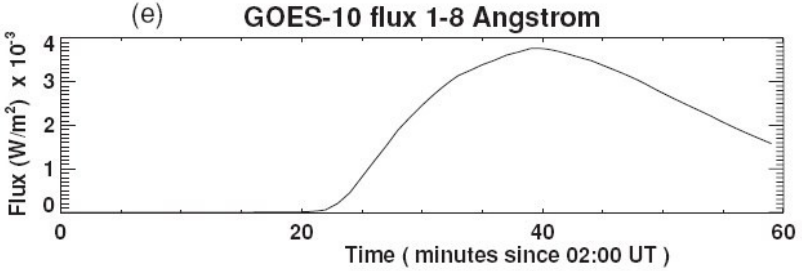
(e)
GOES-10 flux 1-8 Angstrom
Flux (W/m2) x 10-3
Time (minutes since 02:00 UT)

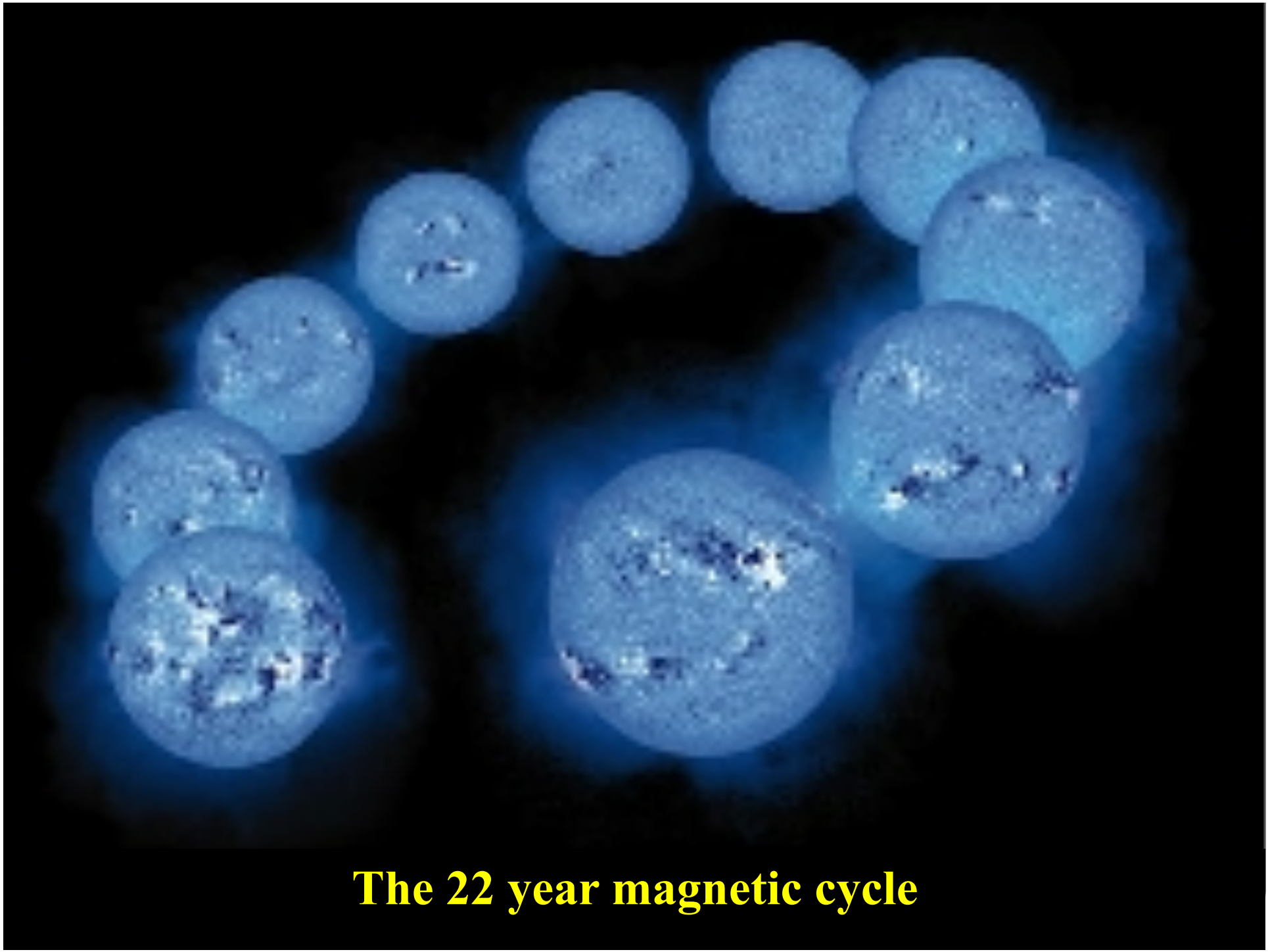

The 22 year magnetic cycle

Some problems, some solutions

Helioseismic Inversion

↓

Large $\frac{d\Omega}{dr}$ in TACHOCLINE

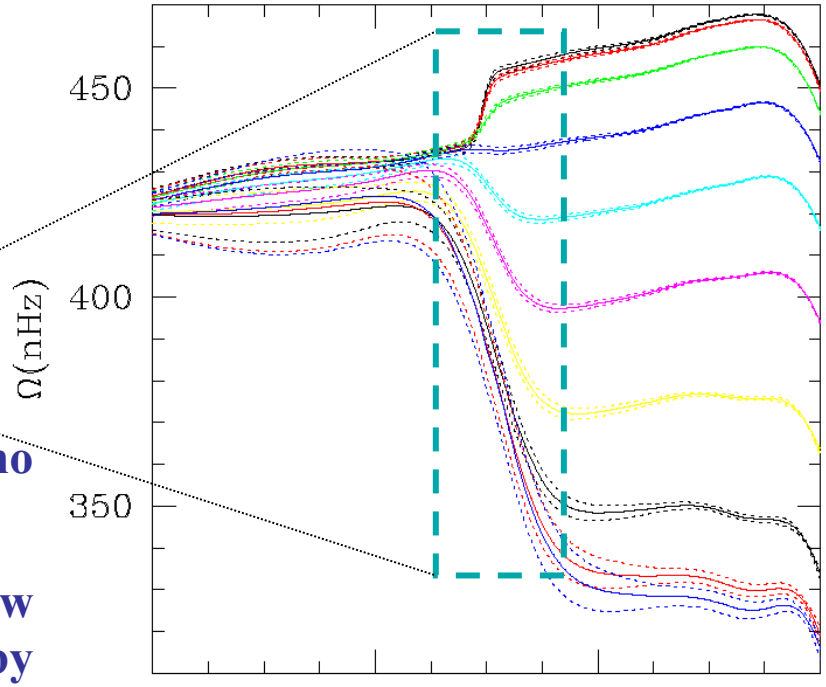

BUT.. $\alpha \frac{d\Omega}{dr} \leq 0$ **as required for Parker's dynamo mechanism is violated in the tachocline……**

Also, Choudhuri's mechanism for Joy's law requires strong fields that cannot be distorted by the eddies at the tachocline

Transport of surface fields should generate poloidal field

Observed polar flux at solar minimum is a good predictor for toroidal flux of next cycle maximum

But observed toroidal flux does not predict the poloidal flux of the next minimum. **Missing flux? OR Missing Dynamo? (e.g.shallow dynamo with topological pumping)**

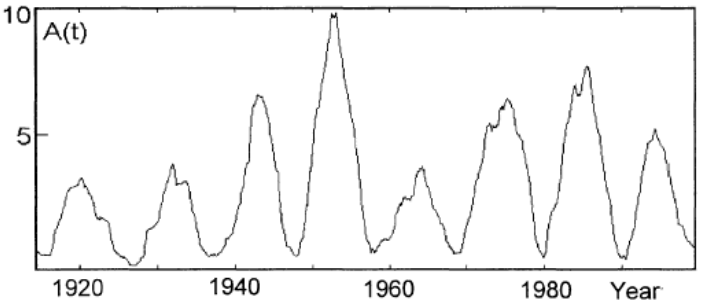

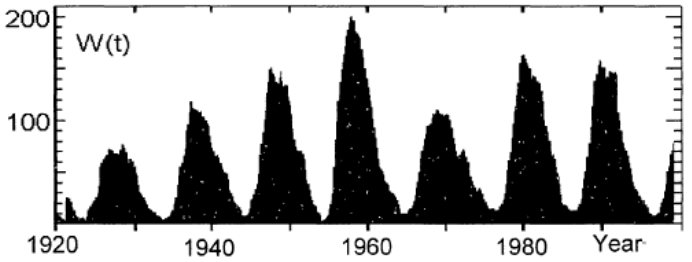

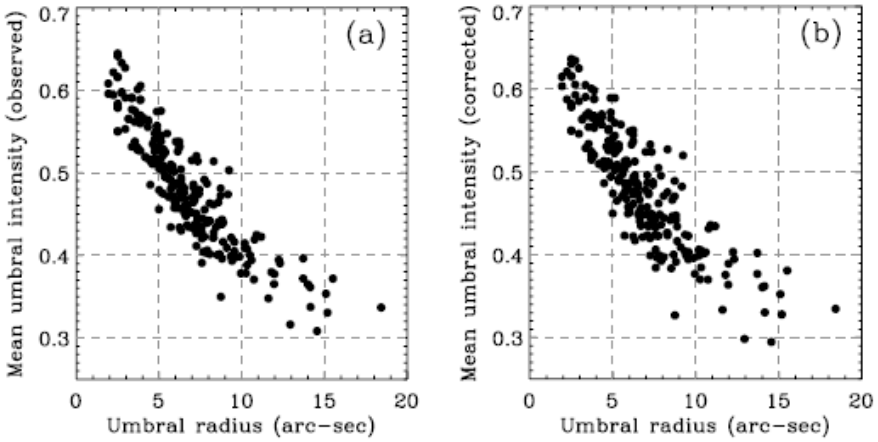

Fig. 11. Mean umbral intensity versus umbral radius, **a)** observed and, **b)** corrected for stray light and the influence of the Ni I line. Here sunspots with umbral radius less than 5 arcsec and greater than 15 arcsec are also included.

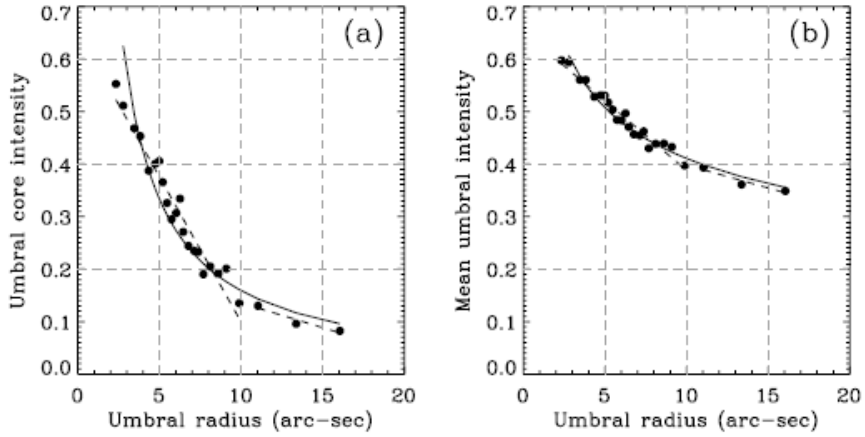

Fig. 12. Power law fit (solid line) and double linear fit (dash lines) to the **a)** umbral core intensity and, **b)** mean umbral intensity. Here the filled circles represent bins of 10 spots each.